UAH Research Report No. 151

A NUMERICAL CALCULATION OF OUTWARD PROPAGATION OF SOLAR DISTURBANCES

by

S. T. Wu and S. M. Han

Final Technical Report

This research work was supported by
the National Aeronautics and Space Administration
George C. Marshall Space Flight Center
Contract NAS8-25101

The University of Alabama in Huntsville
School of Graduate Studies and Research
P. O. Box 1247
Huntsville, Alabama 35807

February 1974

(NASA-CR-120368) A NUMERICAL CALCULATION OF OUTWARD PROPAGATION OF SOLAR DISTURBANCES Final Report (Alabama Univ., Huntsville.) 88 p HC $7.50 N74-32239
Unclas
CSCL 03B G3/29 17050

ACKNOWLEDGEMENT

The authors gratefully appreciate the advice and consultation given by Dr. Y. Nakagawa, High Altitude Observatory, National Center for Atmospheric Research, during the course of this study.

The work was performed with the technical coordination of Dr. M. J. Hagyard, Electromagnetic and Solid State Physics Division, Space Sciences Laboratory, National Aeronautics and Space Administration, Marshall Space Flight Center. Her consultation and encouragement during the course of this study are highly appreciated.

Finally, not the least, I wish to express my thanks to Mrs. Carol Holladay for her patience in typing this manuscript and compiling some of the records.

SUMMARY

In this contract (NAS8-25101), a systematic theoretical investigation of the dynamical behavior of the solar active region has been performed. As a result of these studies, we have concluded that the most appropriate physical mechanism in helping to understand the disturbed solar atmosphere is the propagation of shock waves in a model solar atmosphere. During the course of this contract, we have examined two important cases:

(i) The Downward Propagation and Response of the Chromosphere

In this study, we have examined the responses of the solar chromosphere to an infalling material stream resulting from the "disparition brusque" of a prominence. We found that the solar chromosphere is heated by the shock resulting from the infalling material stream and radiation is enhanced. The enhanced radiation terminates the shock around the height of the temperature minimum in the Harvard-Smithsonian Reference Atmosphere model. This radiation enhancement is identified as Optical (H_α) flares. The detail of this study was submitted to the National Aeronautics and Space Administration, Marshall Space Flight Center, as an Interim Report for this contract, dated March 1972 (UARI Research Report No. 114). A part of this study is also published in Solar Physics, Vol. 30, Page 111-120, 1973.

(ii) The Upward Propagation of Solar Disturbance and Its Responses

After completion of the study of the downward propagation of a shock through the chromosphere (from ~ 2000 Km to the sun's surface), we felt it logical to examine the responses of the solar atmosphere due to an outward propagation shock. Therefore, in this final research report, we shall report the results of this study, since the other results have been documented already. In this study, we have employed the Lax-Wendroff method to solve the set of non-linear partial differential equations, because the method of characteristics used to analyze the downward propagating shock became invalid due to non-homogeneity in the model of the solar atmosphere. It was found that this theoretical model can be used to explain the solar phenomena of surge and spray. A criterion to discriminate the surge and spray was found. The detailed information concerning the density, velocity, and temperature distribution with respect to the height and time is presented. The complete computer program is also included in this report.

Finally, we would like to summarize the publications and research reports resulting from this contract as follows:

i. Refereed Publications

(1) "A Kinematic Model of a Solar Flare," Solar Physics, Vol. 30, 111-120, 1973.

(2) "Non-Equilibrium Ionized Blast Wave," J. of Physical Soc. Japan, Vol. 36, No. 1, 1974.

(3) "Kinetic Description of Solar Wind Interaction with 'Small' Celestial Objects," Rarefied Gas Dynamics (ed. K. Karamcheti), Academic Press, New York, 1974.

(4) "A Kinematic Model of Surge and Spray," to appear in Solar Physics, 1974.

ii. Research Report

"Propagation of Downward Shock Waves Generated by Infalling Dense Prominence Materials in a Realistic Solar Atmosphere," UARI Research Report No. 114, March 1972.

TABLE OF CONTENTS

CHAPTER I
INTRODUCTION

During previous studies [1, 2], we found that the optical (H_α) flare can be identified with the response of the solar chromosphere to a shock wave propagating downward through the chromosphere. The shock wave is related to an infalling material stream resulting from the "disparition brusque" of a prominence as suggested by Hyder [3, 4, 5], and Nakagawa and Hyder [6]. In the general impact theory, there are always two waves generated propagating in opposite directions right at the moment of the impact. According to the coordinate system which we adopted here, one of these two waves is propagating downward through the chromosphere to the photosphere, and another one is propagating upward through the transition region to the corona and beyond. The study of a downward propagating shock through the chromosphere has been completed and reported [1, 2]. Therefore, we shall present the results of upward propagating disturbances (either shocks or subsonic disturbances) through a model solar atmosphere in this report.

To calculate the downward propagating shock through the chromosphere, we have used the CCW (Chisnell, Chester, Whitham) [7] approximation which is based on the theory of characteristics. However, it is noted by Bird [8] that this method of approximation has only provided satisfactory accuracy for a shock propagating into a denser medium. Therefore, it seems to us that it is not quite proper to apply the CCW

approximation to calculate the outward propagating disturbances, because the model solar atmosphere is attenuated outward. Thus, we have chosen the Lax-Wendroff method [9, 10] for the present study. This is a numerical method, which has the advantage of taking care of both the sub- and supersonic disturbances. The numerical accuracy can be controlled by using proper numerical techniques, such as by specifying the proper time increament and grid size in the computation processes based on the physical model of the solar atmosphere.

In this study, the evolution of the disturbances, originating at ~ 30,000 Km (~ 0.0428 R_s R_s being the solar radius ~ 7×10^5Km), is examined in detail using the method we mentioned in the previous paragraph. These disturbances are identified as pressure pulses with different strengths and durations. From the present results, we have shown that the short duration (few minutes) and moderate strength pressure pulse ($\Delta p \sim 2$) will result in the phenomenon of "surge," because it shows that a stream velocity of ~100 - 200 km/sec can be achieved in this case. It also demonstrated that there is an essential part of the material falling back to the sun's surface which agrees with the observation. The longer duration (i.e., 20-40 minutes) and stronger strength pressure pulse ($\Delta p \sim 10$) shows that a stream velocity of the order of 1000 km/sec is achieved and no falling materials can be seen. Thus, we have identified this case as the "spray".

Finally, we should point out, that there is little difference between the adiabatic calculation and the calculation with a Cox-Tucker type

radiation loss as has been shown in the calculation of the downward propagating case [1]. This is because the Cox-Tucker [11] radiative loss is mainly based on the hydrogen-equilibrium radiative-equilibrium estimation that only covers radiation such as the Balmer series. It is worthwhile to examine the radiative effects in further detail.

CHAPTER II

FORMULATION OF THE PROBLEM

II-1 Hydrodynamics Model

In the solar atmosphere of interest in the present study, the gyro-radius is ~ 10 km, and while the scale height is of the order of a thousand kilometers, we can consider that the medium is filled with collision-dominated plasma. Thus, the physical behavior of this plasma can be considered as a continuum fluid. Consequently, the hydrodynamic model was chosen for the present problem.

In dealing with radiative cooling effects in this problem, we have chosen the Cox-Tucker model [11], because the dominating radiation in this part of the solar atmosphere results from bremsstreahlung, recombination radiation, and collision-induced line emission. A summary of this radiative loss is shown in Figure 1. For the convenience of the numerical calculation, a simple, analytical closed-form expression is adopted,

$$Q_R = \chi \rho^2 T^{\alpha} . \qquad (2\text{-}1)$$

The symbol Q_R is the radiative cooling rate (ergs/cm^{3}sec), ρ is the gas mass density (gm/cm^3) and T is the temperature (°K). Finally χ and α constants determined by the results given by Cox and Tucker, as shown in Figure 1. The numerical values for these two constants at various temperatures are presented in Table 1.

Table I. Temperature of Radiative Cooling Rate

Range of Temperature ^{o}K	χ	α
$T \leq 5.0 \times 10^4$	$\chi = 1.0 \times 10^{10}$	$\alpha = 3.55$
$5.0 \times 10^4 < T \leq 2.5 \times 10^5$	$\chi = 3.0 \times 10^{26}$	$\alpha = 0$
$2.5 \times 10^5 < T \leq 7.0 \times 10^6$	$\chi = 1.0\ E^{32}$	$\alpha = -1.172$
$7 \times 10^6 < T$	$\chi = 1.0 \times 10^{23}$	$\alpha = 0.288$
	gives $Q = \chi \rho^2 T^{\alpha}$ (ergs/cm^{3}sec)	

As we have discussed previously, the hydrodynamic model can be used for the present study. In order to avoid unnecessary complexity while retaining the basic physical process of the problem, we consider the plasma flow guided upward along a vertical magnetic flux tube. The possibility of such a confinement is discussed by Nakagawa and Hyder [12], and it was shown that confinement is possible when the gas pressure within the plasma flow is smaller than the local magnetic pressure, i.e.,

$$\frac{B^2}{8\pi} > \frac{2\gamma}{\gamma+1} M^2 p , \qquad (2-2)$$

where B is the strength of magnetic field induction, γ the ratio of specific heats, M the shock Mach number and p the gas pressure. If we consider that the maximum gas pressure in the model of the solar atmosphere is $\sim 1.5 \times 10^{-1}$cgs, which corresponds to the gas flow velocity of the order of 4×10^2 Km/sec, we find that Eq. (2-2) is satisfied for $B \geq 60G$, which is a reasonable value of B in an active region. Therefore, the magnetic force effect can be ignored in this calculation. The governing equations for the present problem can be written as

Continuity:

$$\frac{\partial \rho}{\partial t} + \nabla \cdot (\rho \vec{V}) = 0 \ , \tag{2-3}$$

Momentum:

$$\rho \frac{\partial \vec{V}}{\partial t} + \vec{V} \cdot \nabla \vec{V} = - \nabla p + \rho \vec{g} \ , \tag{2-4}$$

Energy:

$$\rho \frac{\partial \varepsilon}{\partial t} + (\vec{V} \cdot \nabla) \varepsilon = -p \nabla \cdot \vec{V} + \nabla (K \nabla T) - Q_R \tag{2-5}$$

where $\vec{V}$ is the flow velocity and $\vec{g}$ is the gravitational acceleration along the normal axis from the sun's surface, toward the sun. ε is the internal energy of the gas per unit volume, K is the thermal conductivity and Q_R is the radiative cooling loss rate given by Eq. (2-1). Finally the equation of state is

$$p = \rho R T = \rho \frac{k}{m} T \ , \tag{2-6}$$

and

$$E = C_V T = \frac{p}{\rho(\gamma - 1)} \ , \tag{2-7}$$

with R, k, m, and C_V being the gas constant, Boltzmann constant, average molecular weight and specific heat at constant volume, respectively.

Let us adopt the spherical coordinates for the present study, and further assume that the case of spherical symmetry, the thermal conduction is negligible compared with radiation. The Eqs. (2-3) through (2-5) become

$$\frac{\partial \rho}{\partial t} + \frac{\partial}{\partial r} (\rho u) + \frac{2 \rho u}{r} = 0 \tag{2-8}$$

$$\frac{\partial u}{\partial t} + u \frac{\partial u}{\partial r} = - \frac{1}{\rho} \frac{\partial p}{\partial r} - g, \tag{2-9}$$

$$\frac{\partial \varepsilon}{\partial t} + u \frac{\partial \varepsilon}{\partial r} = \frac{p}{\rho} \left(\frac{\partial \rho}{\partial t} + u \frac{\partial \rho}{\partial r} \right) - Q_R , \tag{2-10}$$

where u represents the radial velocity and depends on radius r and time t .

The gravitational acceleration g is given by

$$g = \frac{g_s R_s^2}{r^2} , \tag{2-11}$$

with g_s being the gravitational acceleration at the surface of the sun, and R_s being the solar radius.

Eq. (2-8) through (2 - 10) are set of non-linear time dependent partial differential equations without dispersion coefficients (i.e., viscosity, diffusivity, etc.). To find an analytical solution for this set of equations with various boundary conditions is impossible. However, it is possible to obtain a numerical solution. Some discussion on the existing numerical method will be given in the next chapter.

II-2 Initial and Boundary Conditions

II-2-1 Initial Conditions

Initially, we have assumed the solar atmosphere at the photosphere and chromosphere to be the Harvard-Smithsonian Reference Atmosphere (HSRA) [13]. Beyond its range, the solar atmosphere is assumed to be in a state of hydrostatic equilibrium, which can be calculated from Eq. (2-4), thus

$$\frac{dp^o}{dr} = - \rho^o g = - \rho^o g_s R_s^2 / r^2 , \tag{2-12}$$

where superscript o denotes the quantities at steady state.

Substituting $p^o = \rho^o R T^o$ into (2-12), we obtained

$$\frac{d\rho^o(r)}{dr} = -\rho_o^o(r)\left[\frac{g_s R_s^2}{RT^o(r)}\frac{1}{r^2} + \frac{1}{T^o(r)}\frac{dT^o(r)}{dr}\right] \tag{2-13}$$

Eq. (2-13) should be numerically integrated for a given temperature profile of the atmosphere. However for an isothermal atmosphere Eq. (2-13) reduces to a simpler form

$$\frac{1}{\rho^o}\frac{d\rho^o}{dr} = -\frac{g_s}{RT^o}\frac{R_s^2}{r^2} . \tag{2-14}$$

Integration of this equation yields the solution for the density profile of the hydrostatic atmosphere,

$$\rho^o = \rho_o^o \text{ Exp } \left[\frac{g_s R_s^2}{RT^o}\left(\frac{1}{r} - \frac{1}{r_1}\right)\right] , \tag{2-15}$$

where ρ_o^o is the reference density at $r = r_1$. Steady state pressure distribution is then

$$p^o = p_o^o \text{ Exp } \left[\frac{g_s R_s^2}{RT^o}\left(\frac{1}{r} - \frac{1}{r_1}\right)\right] , \tag{2-16}$$

where p_o^o is the pressure at $r = r_1$.

II-2-2 Boundary Conditions

There are two boundary conditions, one at $r = 0$ and one at $r \to \infty$, to be given. The lower boundary condition will be characterized by disturbances such as density pulse, temperature pulse, velocity pulse, and pressure pulse. To introduce these pulses, we can specify them by prescribing the amplitude and duration of the pulse which depends on the characteristics of the disturbances.

For example, the disturbance is introduced at the lower boundary as a pressure pulse and the velocity is zero at $t = 0$. But, the velocity on the boundary for $t > 0$ will be determined from the continuity equation thus

$$u_1^n = \rho_2^n u_2^n / \rho_1^n \qquad (2\text{-}17)$$

where subscript 1 denotes the boundary and 2 denotes the mesh point next to the boundary, superscript n denotes the time increment, such that $t = n\Delta t \leq \tau$, τ being the duration of the disturbance. When $t > \tau$, disturbance is gone, and the lower boundary returns to its unperturbed condition, i.e., a hydrostatic equilibrium state.

On the upper boundary we have used the completely absorbed condition, i.e., all the effects due to reflected waves are ignored. The reason for keeping this assumption is because the time for the reflected wave to reach the upward-propagating wave packet is much longer than the time for the upward-propagating wave to reach the upper boundary. Thus, the non-reflective boundary condition for velocity can be expressed as

$$\phi_j^n = 2\phi_{j-1}^n - \phi_{j-2}^n \qquad (2\text{-}18)$$

where ϕ represents a physical quantity, the subscript j denotes the mesh points at upper boundary and superscript n denotes the time step.

CHAPTER III

NUMERICAL TECHNIQUE

Numerical computation of time dependent inviscid, compressible flow is a formidable task because of the appearance of discontinuities in the flow field. The conventional way to solve hyperbolic types of differential equations is the method of characteristics. In this method partial differential equations are usually written in characteristic form. Due to the presence of discontinuities in the fluid, these characteristic equations can not be integrated over the entire region of space. Instead, the integral form of the differential equations is used for the discontinuities while differential equations are applied to the remaining region. Although this method is very simple in principle, its application to practical problems is very lengthy and cumbersome. Furthermore, the fact that one cannot know the time and location of such discontinuities in flow field prior to the computation makes application to actual problems almost impractical. Watts and Rosenverg, et.al. [14] solved the transient adiabatic compressible fluid flow in a duct by using the characteristic method in an elegant manner. Their method can be, in principle, extended to solve the present problem. However, the resulting computational procedures will be too complicated to be practical. It may be worthwhile to examine this method in some detail at a later date. Gentry, et al., [15] used the FLIC method, known as Fluid in Cell, to describe the time dependent equations of motion for the compressible flow of a fluid. This method has

been used to solve a wide variety of problems in compressible fluid flow. Hundhausen, et al, [16] used this method to simulate the flare generated disturbances in the solar wind.

Currently, the most commonly adopted method for solving the compressible fluid flow problem is probably the Lax-Wendroff difference method. Lax-and Wendroff [9, 10] suggested that partial differential equations are first written in divergence free form, and then the difference equations in the divergence free form can be generated from these equations. The mathematical proofs are beyond the present scope of these studies and will not be presented in this report. However, the basic idea of this method is that errors caused by the discretization process tend to smooth the solution. This allows the representation of shocks by smearing discontinuities over several mesh points.

There are many versions of the difference scheme for the conservational form of equations. Some detailed comparisons among these versions are made by Ehmery [17] and Burstein [18, 19]. One version due to Burstein [20], is used for the present study.

III-1 Conservational Form of Equations

Divergence-free form of the governing equations will not create or eliminate any flow variables. After some algebraic manipulation (see Appendix A) the governing equations [2-8], [2-9], and [2-10] can be written in Eulerian pseudo-conservational form;

$$\frac{\partial \rho}{\partial t} = -\frac{\partial}{\partial r}(\rho u) - \frac{2\rho u}{r}, \tag{3-1}$$

$$\frac{\partial(\rho u)}{\partial t} = -\frac{\partial}{\partial r}\left[(\gamma-1)\,E - \frac{(\gamma-3)}{2}\,\rho u^2\right] - \rho g - \frac{2\rho u^2}{r} \tag{3-2}$$

$$\frac{\partial E}{\partial t} = -\frac{\partial}{\partial r}\left[u\left(\gamma E - \frac{(\gamma-1)}{2}\,\rho u^2\right)\right] - \rho u g - Q_R - \frac{2}{r}\left[u\left(\gamma E - (\gamma-1)\,\frac{\rho u^2}{2}\right)\right], \tag{3-3}$$

where E is the total energy per unit volume, given by

$$E = \frac{p}{\gamma-1} + \frac{\rho u^2}{2}. \tag{3-4}$$

Using vector notation, Eqs. (3-1), (3-2) and (3-3) can be put in the form

$$\frac{\partial \underset{\sim}{U}}{\partial t} = -\frac{\partial \underset{\sim}{F}}{\partial r} + \underset{\sim}{K} \tag{3-5}$$

where $\underset{\sim}{U}$, $\underset{\sim}{F}$ and $\underset{\sim}{K}$ are three components vectors;

$$\underset{\sim}{U} = \begin{bmatrix} \rho \\ \rho u \\ E \end{bmatrix}, \tag{3-6}$$

$$\underset{\sim}{F} = \begin{bmatrix} \rho u \\ (\gamma-1)E - \frac{(\gamma-3)}{2}\,\rho u^2 \\ u\left(\gamma E - \frac{(\gamma-1)}{2}\,\rho u^2\right) \end{bmatrix}, \tag{3-7}$$

$$\underset{\sim}{K} = \begin{bmatrix} \frac{2\rho u}{r} \\ -\rho g - \frac{2\rho u^2}{r} \\ -\rho u g - Q_R - \frac{2}{r}\left[u\left(\gamma E - (\gamma-1)\frac{\rho u^2}{2}\right)\right] \end{bmatrix} \qquad (3\text{-}8)$$

Using the difference operator, Equation (3-5) is approximated by

$$\delta_t \underset{\sim}{U} = -\delta_r \underset{\sim}{F} + \underset{\sim}{K}, \quad \text{where} \qquad (3\text{-}9)$$

δ_t and δ_r is yet to be discussed. There are several versions of Lax-Wendroff difference schemes which have been extensively used for a wide range of fluid flow problems.

Lax-Wendroff scheme is based on the Taylor series expansion of the vector function $\underset{\sim}{U}(r, t + \Delta t)$ so as to include the second order term $\partial^2\underset{\sim}{U}/\partial t^2$. A two-step method obtained by Richtmyer [21] is used here. The values at the intermediate points are computed at a time $t + \Delta t/2$ using a first-order correct scheme, and then a second-order correct scheme (leap frog) is used to compute the value at time $t + \Delta t$. The overall scheme has, then a second-order correct differencing scheme. Burstein, et. al. [20] suggested that instead of computing the intermediate value at time $t + \Delta t/2$, they compute them at $t + \Delta t$ and then average the F difference at t and $t + \Delta t$ so that both the $\underset{\sim}{U}$ and $\underset{\sim}{F}$ values are centered at point $(i, t + \Delta t/2)$. The above differencing method applied to Equation (3-5) yields the following difference approximation:

Intermediate Values

$$\left.\begin{aligned}
\bar{\underset{\sim}{U}}^{n+1}_{i+1/2} &= \frac{1}{2}\left(\underset{\sim}{U}^{n}_{i+1} + \underset{\sim}{U}^{n}_{i}\right) - \frac{\Delta t}{\Delta x}\left(\underset{\sim}{F}^{n}_{i+1} - \underset{\sim}{F}^{n}_{i}\right) + \frac{\Delta t}{2}\left(\underset{\sim}{K}^{n}_{i+1} + \underset{\sim}{K}^{n}_{i}\right) \\
\bar{\underset{\sim}{U}}^{n+1}_{i-1/2} &= \frac{1}{2}\left(\underset{\sim}{U}^{n}_{i} + \underset{\sim}{U}^{n}_{i-1}\right) - \frac{\Delta t}{\Delta x}\left(\underset{\sim}{F}^{n}_{i} - \underset{\sim}{F}^{n}_{i-1}\right) + \frac{\Delta t}{2}\left(\underset{\sim}{K}^{n}_{i} + \underset{\sim}{K}^{n}_{i-1}\right) \\
\bar{\underset{\sim}{U}}^{n+1}_{i} &= \frac{1}{2}\left(\underset{\sim}{U}^{n}_{i-1} + \underset{\sim}{U}^{n}_{i+1}\right) - \frac{\Delta t}{2\Delta x}\left(\underset{\sim}{F}^{n}_{i+1} - \underset{\sim}{F}^{n}_{i-1}\right) + \Delta t\, \underset{\sim}{K}^{n}_{i}
\end{aligned}\right\} \quad (3\text{-}10)$$

where the bar signifies the intermediate flow variables at $(i-1/2)\Delta x$, $i\Delta x$, $(i+1/2)\Delta x$ and at $(n+1)\Delta t$. Using these intermediate values of the variables we calculate the final values.

Final Values

$$\underset{\sim}{U}^{n+1}_{i} = \underset{\sim}{U}^{n}_{i} - \frac{\Delta t}{2\Delta x}\left[\frac{1}{2}\left(\underset{\sim}{F}^{n}_{i+1} - \underset{\sim}{F}^{n}_{i-1}\right) + \left(\bar{\underset{\sim}{F}}^{n+1}_{i+1/2} - \bar{\underset{\sim}{F}}^{n+1}_{i-1/2}\right)\right] + \frac{\Delta t}{2}\left(\underset{\sim}{K}^{n}_{i} + \bar{\underset{\sim}{K}}^{n+1}_{i}\right), \quad (3\text{-}11)$$

where the intermediate values of $\bar{\underset{\sim}{F}}^{n+1}_{i+1/2}$, $\bar{\underset{\sim}{F}}^{n+1}_{i-1/2}$ and $\bar{\underset{\sim}{K}}^{n+1}_{i}$ are calculated by using Eqs. (3-7) and (3-8) with intermediate flow variables obtained in the previous step. Combining Eqs. (3-10) and (3-11), it is easily seen that this is a second-order correct-differencing scheme.

III-2 Numerical Stability

Finite difference equations may exhibit rapidly growing and oscillatory solution that cannot resemble the true solutions of partial differential equations. In this case, the difference equation is said to be computationally unstable. The origin of instabilities varies with a particular set of partial differential equations. Many theories and criteria have been developed by many investigators, such as Richtmyer and Morton [22], Hirt [23], and Van Leer [24]. However, it is not possible to have a general theory for higher-order non-linear equations, such as in the present problem. The discussion given here is not rigorous, but presents some heuristic techniques which prove very useful in stabilizing the computations.

III-2-1 Time Interval

As a first approximation, the time interval for successive interations can be found by applying the stability criterion of Courant, Friedrichs and Lewy,

$$\Delta t_s < \frac{\Delta r}{|u| + a} , \qquad (3\text{-}12)$$

where a is the local sound speed. When a thermal conduction term is included in the governing equations, thermal conduction stability criteria should be considered. Applying the Fourier method proposed by von Neumann concerning the heat conduction equation, one finds the time interval [5] Δt_c to be

$$\Delta t_c < \frac{\frac{1}{2} p (\Delta r)^2}{K(\gamma-1)T^{7/2}} . \qquad (3\text{-}13)$$

In the case of heat exchange terms becoming arbitrary, namely Q_R, the K_3 vector in Eq. (3-8) of the present problem, can be varied very rapidly. When such a case occurs, numerical oscillation starts and computation terminates. In order to smear out such oscillation, the time step is chosen according to

$$|Q_R| \Delta t_Q < \frac{1}{2} \frac{p}{\gamma-1} . \tag{3-14}$$

For a model that does not include the conduction term, $0.25 \Delta t_s$ is sufficiently small to satisfy all stability criteria.

III-2-2 Artificial Viscosity

If the strength of the disturbance is large, a sharp jump in the flow variable occurs in the flow field. We can find this jump condition by applying the Rankine-Hugoniot relations. In numerical simulation, these discontinuities easily cause the onset of instability. Thus, the artificial viscosity is introduced to help offset the instability. The idea of introducing artificial viscosity into shock calculations is due to the work of von Neumann and Richtmyer [25]. The basic requirements for a purely artificial dissipative term are:

(i) all flow variables should have smooth transitions across the discontinuity;

(ii) transitions should have correct jump conditions computable with Rankine-Hugoniot conditions;

(iii) the discontinuity should travel at very nearly the correct speed; and

(iv) the thickness of transition is independent of shock strength, pressure or density of material while the shock is moving [26].

Introducing a pseudo-viscous pressure term in the compression zone, it is shown that all requirements for the artificial viscosity are satisfied. The pseudo-pressure is given by [26]

$$q = \begin{cases} (\rho \ell^2) \left(\frac{\partial u}{\partial r}\right)^2 & \text{if} \quad \partial u/\partial r < 0 \\ 0 & \text{if} \quad \partial u/\partial r \geq 0 \end{cases} \tag{3-15}$$

where ℓ is a constant having the dimensions of length. Then the total energy, Eq. (3-4), for the compression region, $\partial u/\partial r < 0$, is modified to include the pseudo-pressure, such that

$$E = \frac{p + q}{\gamma - 1} + \frac{\rho u^2}{2} \tag{3-16}$$

It is seen clearly that this correction only affects the compression region and that the continuity equation is inact by this modification. Letting $\ell = \beta \Delta r$, the appropriate difference approximation for the altered pressure is then

$$(p+q)_i^n = \begin{cases} p_i^n + \frac{1}{2} \beta^2 \rho_i^n \left(u_{i+1}^n - u_i^n\right)^2 & \text{if } u_{i+1}^n < u_i^n \\ p_i^n & \text{if } u_{i+1}^n \geq u_i^n \end{cases} \tag{3-17}$$

for the intermediate step, and

$$\overline{(p+q)}_{i+1/2}^{n+1} = \begin{cases} p_i^{n+1} + \frac{1}{2} \beta^2 \rho_{i+1/2}^{n+1} \left(\bar{u}_{i+1}^{n+1} - \bar{u}_{i+1/2}^{n+1}\right) & \text{if } \bar{u}_{i+1}^{n+1} < \bar{u}_{i+1/2}^{n+1} \\ p_i^{n+1} & \text{if } \bar{u}_{i+1}^{n+1} \geq \bar{u}_{i+1/2}^{n+1} \end{cases} \tag{3-18}$$

for the final step of computations, where — signifies the intermediate values, and β has the value of 1 to 5. The effect of q on the overall picture is carefully tested by several trial runs. There is no significant change in flow variables except at discontinuities, and the transition occurred over 3 or 4 mesh points.

III-2-3 Shock Dissipation

Mechanical energy carried by the shock wave is dissipated into thermal energy of the gas which experiences an irreversible, non-isentropic process as the shock front passes through the gas. For a unit mass of gas, the thermal energy increases in terms of enthalpy which depends on how the post shock gas returns to its pre-shock gas state. Schtzmann [27] suggested that the gas expands adiabatically until it comes back to the initial pressure and then cools down until it reaches the initial density. Along this path, the change of enthalpy is given by [28]

$$\Delta h = -\frac{p-p_o}{2}\left(\frac{1}{\rho}+\frac{1}{\rho_o}\right) - \frac{\gamma}{\gamma-1}\left(\frac{p}{\rho}+\frac{p_o}{\rho_o}\right) \tag{3-19}$$

where subscript o denotes the pre-shocked gas. Then, for a periodic disturbance propagation, the total enthalpy change of the gas is

$$Q_D = -\frac{\rho_o}{\omega}\Delta h \tag{3-20}$$

where ω is the period of the disturbance. Letting

$$\psi = \frac{p}{p_o},\quad \sigma = \frac{\rho}{\rho_o} \quad \text{and} \quad \zeta = \left(\frac{\psi}{\sigma}\right)^{1/2},$$

Eq. (3-20) becomes

$$Q_D = - \frac{\rho_o a_o^2}{\omega \gamma} \left[\frac{1}{2} (\psi-1) \left(\frac{1}{\sigma} + 1 \right) - \frac{\gamma}{\gamma-1} (\zeta^2+1) \right] , \qquad (3\text{-}21)$$

where ψ and σ are functions of shock Mach number; that is,

$$\psi = \frac{2\gamma}{\gamma+1} M_s^2 - \frac{\gamma-1}{\gamma+1}$$

$$\sigma = \frac{(\gamma+1) M_s^2}{(\gamma-1) M_s^2 + 2} , \qquad (3\text{-}22)$$

$$M_s = \frac{\text{shock speed relative to pre-shock gas}}{\text{sonic speed in pre-shock gas}} \qquad (3\text{-}23)$$

The detailed structure of the shock front must be known in terms of its position and its strength M_s in order to find the accurate shock dissipation in the gas. However, it is not possible to determine the exact position of the shock front, since the transition occurs over several mesh points. It is not quite clear how to determine the exact shock strength M_s in this numerical calculation. The pressure difference between the neighboring points does not give the shock strength, because the unperturbed solar atmosphere possesses a densiyt gradient. In order to give an approximate shock strength at position $i\Delta r$, the following equation is employed:

$$M_{s_i} = \frac{u_{i-1} - u_i}{a_i} . \qquad (3\text{-}24)$$

This equation only gives a parameter which is related more to the local gas flow than the shock strength. In other words, Eq. (3-24) is a sufficient condition for a shock, but not a necessary one. It does,

however, provide a mechanism for continuously monitoring the presence of the discontinuity, whenever the discontinuity occurs, in a very simple manner. In computation, then, from Eq. (3-21) with Eqs. (3-22) and (3-24), the dissipated energy due to the shock is included in the form

$$(Q_D)_i^n = \begin{cases} -\dfrac{\rho_i a_i^2}{\omega \gamma}\left[\dfrac{1}{2}(\psi_i^n - 1)\left(\dfrac{1}{\sigma_i^n}+1\right) - \dfrac{\gamma}{\gamma-1}\left(\zeta_i^{n^2}+1\right)\right] & \text{for } \psi_i^n \le 1 \\ 0 \end{cases} \quad (3\text{-}25)$$

For a dynamic model, the exact value of ω cannot be defined. An estimation of ω is made on the ground that the weak shock travels one mesh point within the time Δt_s, i.e.,

$$\Delta t_s = \frac{\Delta r}{|u| + a} .$$

Since the Lax-Wendroff method is an explicit difference scheme, disturbances travel one mesh point for each full iteration. Thus, ω equals to Δt_s approximately. Without the addition of Q_D in the K_3 term in equation (3-8), the temperature of the gas just ahead of the shock goes negative sometimes, and the calculation is terminated. With this modification, the solution remained stable and there is no noticeable difference in shock structure.

III-2-4 Minor Modifications on Difference Equations

Due to the exponential decrease of density in a quiet solar atmosphere, the difference scheme needs two minor modifications. For a hydrostatic solar atmosphere, the density variation along the r-direction is from Eq. (2-15),

$$\rho_i^n \simeq \rho_1^n \exp\left(-h_i^n r_i/\Delta r\right), \quad (3\text{-}26)$$

where

$$h_i^n = \frac{g_i}{RT_i^n} \Delta r \quad \text{(scale height)} \tag{3-27}$$

Then the nearest-neighbor average value appearing in the first term in RHS of Equation (3-10) is larger than the value at the central point, i.e.,

$$0.5\left(\rho_{i-1}^n + \rho_{i+1}^n\right) = 0.5\left[\rho_i^n\left(e^{-h_i^n} + e^{\,h_i^n}\right)\right]$$

$$= 0.5\,\rho_i^n\left[2+\left(h_i^n\right)^2\right] = \rho_i^n\left(1+\frac{\left(h_i^n\right)^2}{2}\right) > \rho_i^n \tag{3-28}$$

If this difference is not corrected, the density after the intermediate step will become excessively large, and the unchanged vertical pressure cannot support this excess material. Consequently, a downward velocity appears over the entire field. Instead of a simple average, an expression

$$0.5\left(\rho_{i-1}^n + \rho_{i+1}^n\right) + \left[\rho_i^n - 0.5\left(\rho_{i-1}^n + \rho_{i+1}^n\right)\right]$$

is used for ρ_i^n.

Rearranging this, one gets

$$0.5\left(\rho_{i-1}^n + \rho_{i+1}^n\right) + 0.5\,\rho_i^n\left[1-0.5\left(e^{-h_i^n} + e^{\,h_i^n}\right)\right] \tag{3-29}$$

If the nearest-neighbor points have the same value as the center, then Eq. (3-29) reduces to the simple neighbor-points average value.

In the process of calculation, the 2nd correction term in Eq. (3-29), is applied for the intermediate step of each iteration for all conservational variables at full mesh points.

Due to the exponential variation of the hydrostatic equilibrium state,

the difference approximation is systematically different from the derivatives they approximate. That is why the error grows from Eq. (3-26),

$$\frac{\partial \rho_i^n}{\partial r} = - \frac{h_i^n}{\Delta r} \rho_i^n \tag{3-30}$$

But the simple centered difference approximation to the first derivative with respect to r gives

$$\begin{aligned} \delta_r \rho_i^n &= \frac{\rho_{i-1}^n - \rho_{i+1}^n}{2\Delta r} = \frac{e^{-h_i^n} - e^{h_i^n}}{2\Delta r} \rho_i^n \\ &\approx - \frac{h_i^n}{\Delta r} \left(1 + \frac{\left(h_i^n\right)^2}{6}\right) \rho_i^n < \frac{\partial \rho_i^n}{\partial r} \quad . \end{aligned} \tag{3-31}$$

Unless this discrepancy is corrected, an incorrectly calculated pressure term in Eq. (3-2) will set the flow field in an upward motion. In order to avoid this non-physical situation, a correction term c_i^n is defined such that

$$\left(\delta_r + c_i^n\right) \rho_i^n = \frac{\partial \rho_i^n}{\partial r} \tag{3-32}$$

Combining Equations (3-31) and (3-32), c_i^n is found to be

$$c_i^n = - \frac{1}{\Delta r} \left[h_i^n + 0.5 \left(e^{-h_i^n} - e^{+h_i^n}\right)\right] \tag{3-33}$$

This correction term is included for both steps in each iteration.

III-3 Computation Procedure

The actual calculation procedure for the present problem is illustrated in Figure 2.

The steady state temperature T of the atmosphere is assumed to be known and the steady state density is found by using Eq. (2-15), i.e.,

$$\rho_i^n = \rho_1^n \, \mathrm{Exp}\left[\frac{g_s R_s^2}{R T_i^n}\left(\frac{1}{r_i} - \frac{1}{r_1}\right)\right] . \tag{3-34}$$

For a hydrostatic equilibrium state the velocity of the field is zero,

$$u_i^n = 0 \tag{3-35}$$

The total energy is then, from Eq. (3-16),

$$E_i^n = \frac{p_i^n + q_i^n}{\gamma - 1} + \frac{\left(\rho_i^n u_i^n\right)^2}{2\rho_i^n} , \tag{3-36}$$

where p_i^n and q_i^n are determined by Eqs. (3-17) and (3-18), respectively.

The disturbance at the lower boundary is introduced in terms of a pressure jump. For instance, $\rho_*^n = 2\rho_1^n$, $T_*^n = T_1^n$ will give $p_*^n/p_1^n = 2$. This arbitrary disturbance was kept constant for a prescribed time interval τ. After this period of time, the lower boundary returns to its original state.

The time increment Δt is found by the CFL (Courant-Fredricks-Levy) condition, and is applied to each mesh point in the flow field.

Using these initial values of conservational variables, the fluxes at time ($n\Delta t$) are found from Eq. (3-7) and (3-8).

$$F_{1_i}^n = (\rho u)_i^n$$

$$F_{2_i}^n = (\gamma-1)\, E_i^n - \frac{(\gamma-3)}{2}\, \rho_i^n\, (u_i^n)^2$$

$$F_{3_i}^n = u_i^n \left(\gamma\, E_i^n - \frac{(\gamma-1)}{2}\, \rho_i^n\, (u_i^n)^2 \right)$$

$$K_{1_i}^n = \frac{2\rho_i^n\, u_i^n}{r_i}$$

$$K_{2_i}^n = -\rho_i^n\, g_i - \frac{2\,\rho_i^n\, (u_i^n)^2}{\gamma}$$

$$K_{3_i}^n = -\rho_i^n\, u_i^n\, g_i - (Q_R)_i^n - \frac{2}{r}\left[u_i^n \left(\gamma E_i^n - (\gamma-1)\, \frac{\rho_i^n\, (u_i^n)^2}{2} \right) \right] + (Q_D)_i^n$$

where

$g_i = g_s\, R_s^2 / (r_i)^2$; gravitational acceleration

E_i^n is given by Eq. (3-25).

$$(Q_R)_i^n = -\chi\, \rho_i^n\, (T_i^n)^{\alpha}$$

and $(Q_D)_i^n$ is given by Equation (3-25).

Using these fluxes at $n\Delta t$, the intermediate conservational flow variables at $(n+1)\Delta t$ are found from Eq. (3-10) with Eq. (3-29). Intermediate fluxes at $(n+1)\Delta t$ are found by similar manner as those at $n\Delta t$ except intermediate flow variables, $\bar{\underset{\sim}{U}}_i^n$ should be used in Eq. (3-29) and (3-33). The new flow variables at $(n+1)\Delta t$ are then calculated by using Eq. (3-11) with the aid of Eq. (3-33).

CHAPTER IV

RESULTS OF COMPUTATIONS

Numerical results are obtained for given various initial boundary conditions identified as a pressure pulse with different amplitude and duration resulting from possible solar disturbances due to solar activities. All disturbances are placed at the lower boundary which is located at ~30,000 Km (1.043 R_s) above the sun's surface, and all the calculations are carried out to ~ 3 R_s (R_s being the solar radius). The results obtained in this report are the density, temperature and mass flow velocity as a function of height and time for Δp (pressure disturbance) equal to 2 ~ 10 and $\Delta\tau$ (duration of the disturbances) equal to 30 sec, 60 sec, 120 sec, 1200 sec, and in some cases, 2400 sec. A detailed discussion of these results will follow.

Figure 3a, b, and c plotted the disturbed density, temperature and velocity due to disturbances of $\Delta p = 2$ and $\Delta\tau = 120$ sec. It shows that the disturbance has little effect on temperature and density and its influence on mass flow velocity is significant. It appears that this disturbance has created a mass stream shooting out from the upper chromosphere or/lower corona to upper corona with a flow velocity ~ 50 Km/sec at ~ $1R_s$ from the surface (i.e., ~ $2R_s$ from the center of the sun). Similar plots with different initial strength and duration of disturbances are given in Figures 4a, b, c through 11 a, b, c. These results clearly demonstrate that the characteristics of the disturbances are the essential

parameters of the effects of the disturbed solar atmosphere.

Some general features of the disturbed solar atmosphere can be observed from these results. Namely, the stronger initial disturbance gives a stronger temperature enhancement and its mass flow velocity can reach as high as 1000 Km/sec, and a longer duration of the disturbance will sustain the disturbed solar atmosphere, and there will be material falling back to the sun's surface. For example, we have plotted the velocity versus height for $\Delta p = 6$ and $\Delta\tau$ = 30 sec, 120 sec, 1200 sec, and 2400 sec at t - 40 min. after explosion. This shows that the negative velocities (i.e., downward velocity) appeared near the surface of the sun for $\Delta\tau$ = 30 sec, 120 sec and 1200 sec and for $\Delta\tau$ = 2400 sec, mass flow velocity just ejects out from the sun's surface all the way. From this evidence, we may suggest that the surge develops due to a short duration disturbance, because, observations show the material falling back to the sun's surface during a surge.

Now, we shall calculate the total energy of the disturbance initially introduced into the solar atmosphere. The total energy can be computed from

$$E = \left(\sum_i V_i\right) \frac{p}{\gamma+1} + \frac{1}{2} \left(\sum_i V_i \rho_i u_i^2\right) \qquad (4\text{-}1)$$

where on the right hand side, the first term represents the internal energy and the second term represents the kinetic energy of the gas in a volume $(\sum_i V_i)$. The results corresponding to various disturbances are shown in Table II.

Table II
Total Energy Per Cross-Section Area for Each Disturbance

(ergs/Km^2)

Δp	$\Delta\tau$ = 30 sec	$\Delta\tau$ = 120 sec	$\Delta\tau$ = 1,200 sec	$\Delta\tau$ = 2,400 sec
10	7.31×10^{17}	9.42×10^{18}	3.80×10^{20}	6.72×10^{20}
6	1.98×10^{17}	2.63×10^{18}	1.38×10^{20}	2.76×10^{20}
2	2.60×10^{16}	1.48×10^{17}	1.8×10^{19}	

If we consider the cross-section area of a disturbance which has a radius of ~ 500 Km., it will give a total energy of ~ 5.28×10^{26} ergs for the $\Delta p = 10$ and $\Delta\tau = 2400$ disturbance. This may correspond to the total energy of a class of sub-flare.

From those density profiles, such as Figures 3a, 4a, 5a, 6a, 7a, 8a, 9a, 10a, and 11a, we can estimate the amount of particles which can be ejected into the corona (or solar wind), and the results are given in Table III.

Table III
Total Number Particles Per Cross Sectional Area
for Each Disturbance (#/Km^2)

Δp	$\Delta\tau$ = 30 sec	$\Delta\tau$ = 120 sec	$\Delta\tau$ = 1,200 sec	$\Delta\tau$ = 2,400 sec
10	4.77×10^{26}	5.87×10^{27}	1.87×10^{29}	3.44×10^{29}
6	2.60×10^{26}	3.37×10^{27}	1.42×10^{29}	2.85×10^{29}
2	5.5×10^{25}	7.30×10^{26}	3.43×10^{28}	

Again, if we consider the cross-section area of the disturbance being ~500 Km in radius, we find that 2.7×10^{35} particles can be added to the corona, which is believed by many to be a reasonable number.

From this study, we have shown that the surge and spray can result from disturbances in the solar atmosphere. After the disturbance has been introduced, the corona may settle into a new equilibrium state. Evidence for this has been reported in some of the observations from the ATM/Skylab experiments.

CHAPTER V

CONCLUSION AND RECOMMENDATIONS

In this investigation, we have examined the upward propagating solar disturbances in a model atmosphere. It was found that the characteristics of the disturbances have dominant effects on the disturbed solar atmosphere. We may conclude from this study that the phenomena of surge and spray can be discriminated by the characteristics of the initial disturbance, as we discussed in the previous chapter. Also, the present model can be used to examine the observed X-ray data from the Skylab mission by relating the X-ray emission to the dynamical responses of the solar atmosphere. The initial disturbances introduced in this study can be either subsonic or supersonic without limitations.

The radiation effects on this problem were examined by using the Cox-Tucker radiation loss function. We found that there is no noticeable difference between the adiabatic calculation and the radiative calculation with the Cox-Tucker radiative loss function. This is due to the fact that the radiative loss function given by Cox-Tucker is decreasing as the temperature is increasing. Therefore, it is necessary to calculate the radiative loss energy from the spectral lines in order to have more accurate results. Also, we have ignored the transport effect in the present analysis.

Finally, we shall outline as follows, the steps which should be taken to improve the present analysis:

(1) Include magnetic field in this model calculation.

(2) Include thermal conduction effects.

(3) A detailed radiative hydrodynamic calculation procedure needs to be considered.

REFERENCES

1. S. T. Wu and S. M. Han, "Propagation of Downward Shock Waves Generated by Infalling Dense Prominence Materials in a Realistic Solar Atmosphere," UARI Research Report No. 114, March 1972.

2. Y. Nakagawa, S. T. Wu and S. M. Han, Solar Phys., 30, 111, 1973.

3. C. L. Hyder, Nobel Symposium 9, Mass Motion in Solar Flares, (Ed. Yngve Ohman) John Wiley and Sons, 1968.

4. C. L. Hyder, Solar Phys. 2, 49, 1967.

5. C. L. Hyder, Solar Phys. 2, 267, 1967.

6. Y. Nakagawa and C. L. Hyder, Environmental Research Paper No. 320, AFCRL-70-0273, 1970.

7. G. B. Whitham, J. Fluid Mech. 4, 337, 1958.

8. G. A. Bird, J. Fluid Mech., 11, 180, 1961.

9. P. Lax and B. Wendroff, Comm. on Pure and Applied Math., 13, 217, 1960.

10. P. Lax and B. Wendroff, Comm. on Pure and Applied Math., 17, 381, 1964.

11. D. P. Cox and W. H. Tucker, Astrophys. J. 157, 1157, 1969.

12. Y. Nakagawa and C. L. Hyder, Private Communication.

13. O. Gingerich, R. W. Noyes, W. Kalkofen, and Y. Cuny, Solar Phys. 18, 347, 1971.

14. J. W. Watts and D. U. Rosenverg, Chemical Eng. Sci., 24, 49, 1969.

15. R. A. Gentry, R. E. Martin, and B. J. Daly, J. of Comp. Phys. 1, 87, 1966.

16. A. J. Hundhausen and R. A. Gentry, J. of Geophys. Res., 74, 2908, 1969.

17. A. F. Emery, J. of Comp. Phys., 2, 306, 1968.

18. S. Z. Burstein, AIAA J. 2, 2111, 1964.

19. S. Z. Burstein, J. of Comp. Phys. 2, 198, 1967.

20. S. Z. Burstein, J. of Comp. Phys. 2, 178, 1967.

21. R. D. Richtmyer, NCAR Tech. Note, 63-2, 1963.

22. R. D. Richtmyer and K. W. Morton, NYO 1840-5, August 1964.

23. C. W. Hirt, J. of Comp. Phys., 2, 339, 1968.

24. B. vanLeer, J. of Comp. Phys., 3, 473, 1969.

25. J. von Neumann and R. D. Richtmyer, J. of Applied Phys., 21, 232, 1950.

26. R. D. Richtmyer and K. W. Morton, Difference Methods for Initial-Value Problem, Interscience Publishers, New York, 1967.

27. E. Shatzmann, Solar Astronomy (Ed. J. N. Xanthakis) Interscience Publishers, London, 1963.

LIST OF FIGURES

Radiative Cooling Rate of an

Optically Thin, High Temperature Plasma

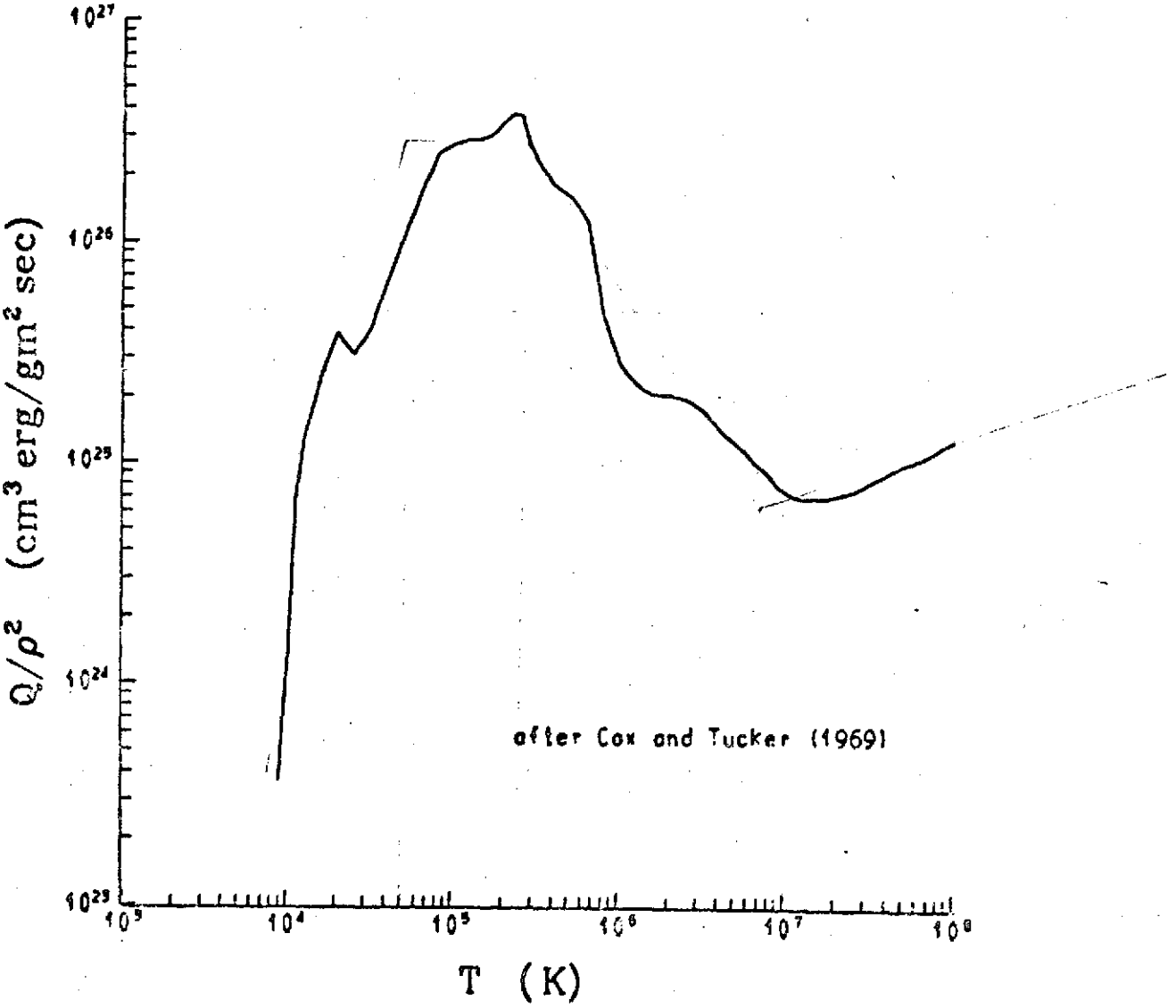

FIGURE 1

FIGURE 2. FLOW DIAGRAM

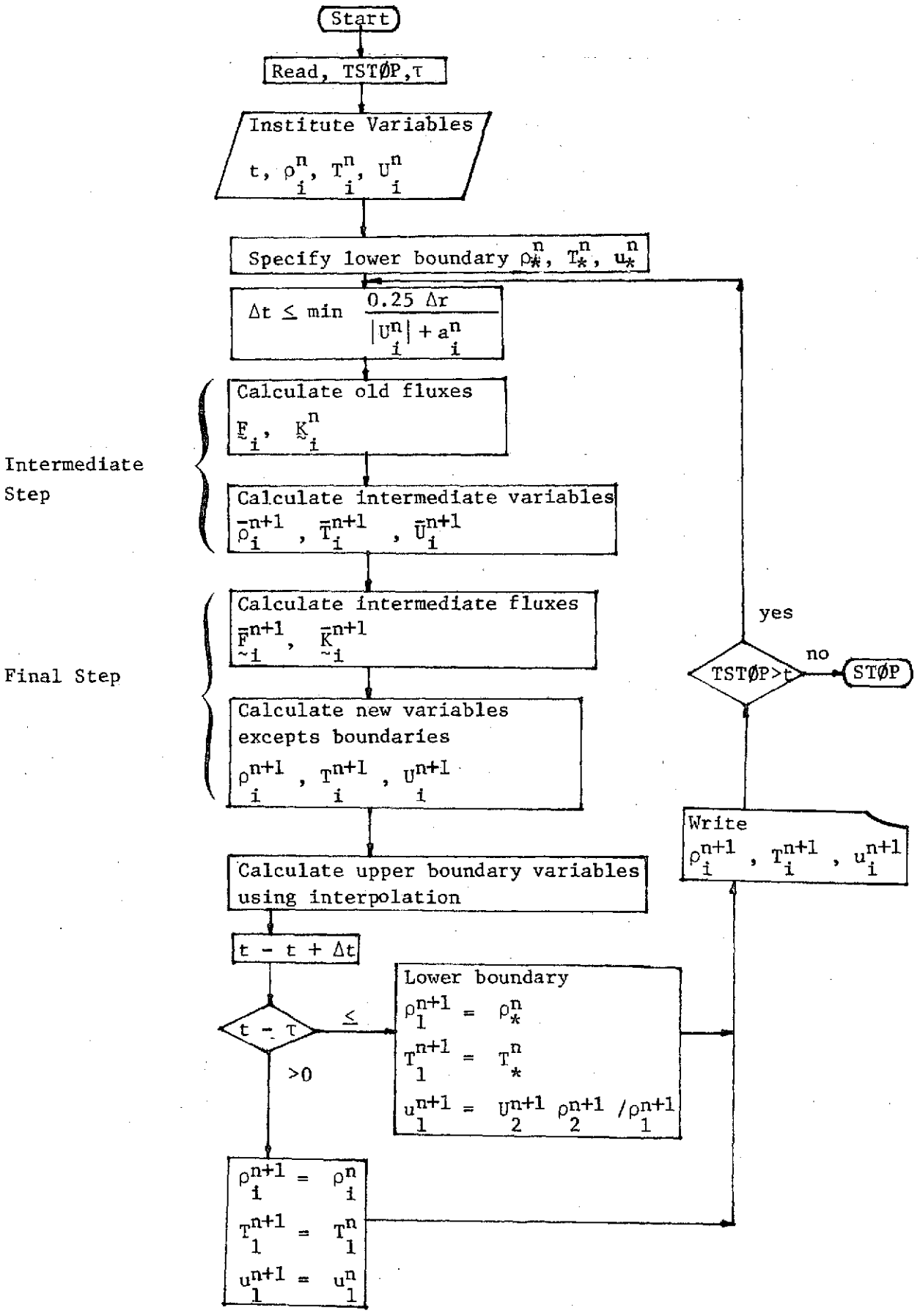

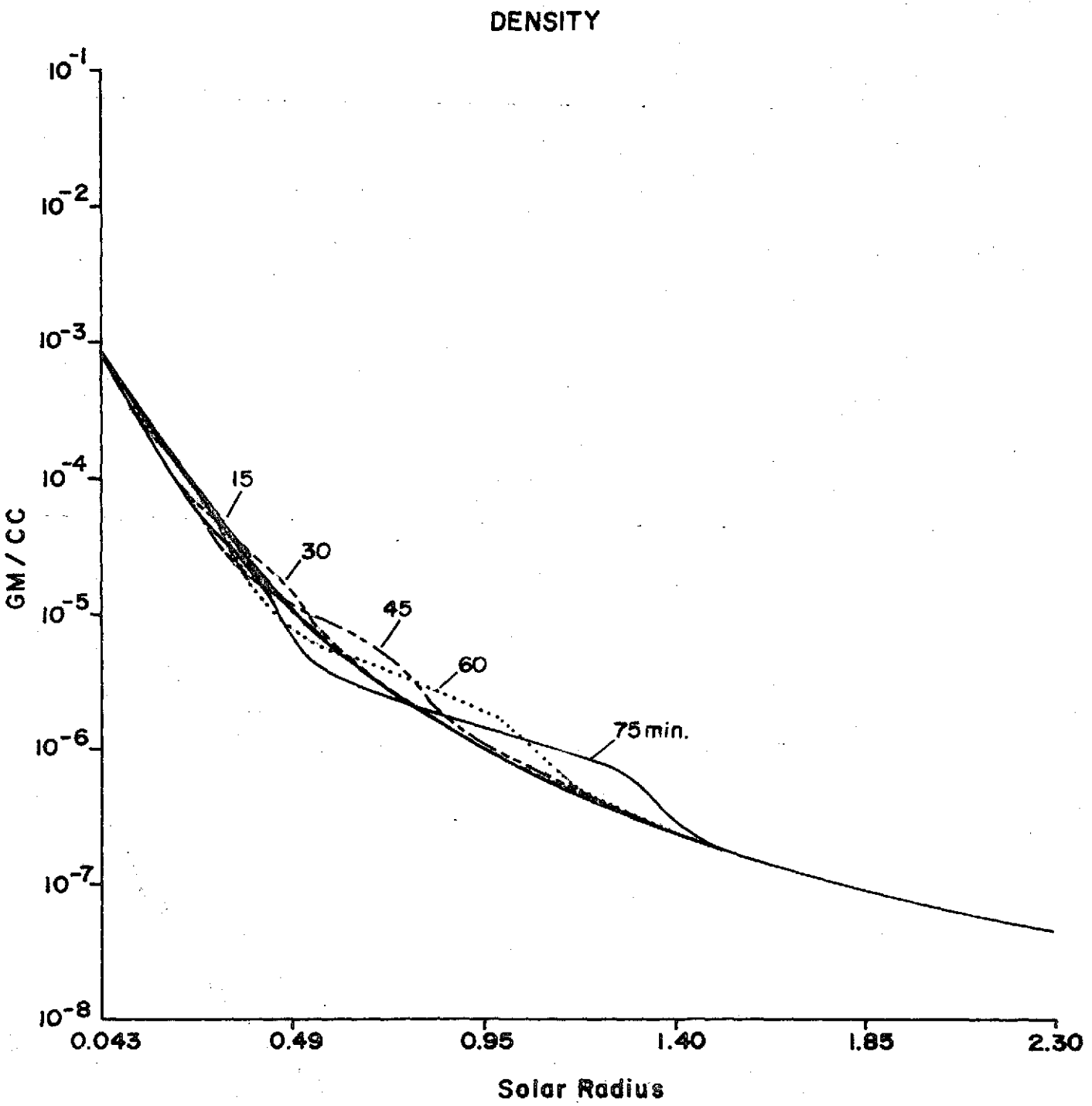
DENSITY
10^{-1}
10^{-2}
10^{-3}
10^{-4}
10^{-5}
10^{-6}
10^{-7}
10^{-8}
GM / CC
15
30
45
60
75 min.
0.043
0.49
0.95
1.40
1.85
2.30
Solar Radius

FIG. 3 - a

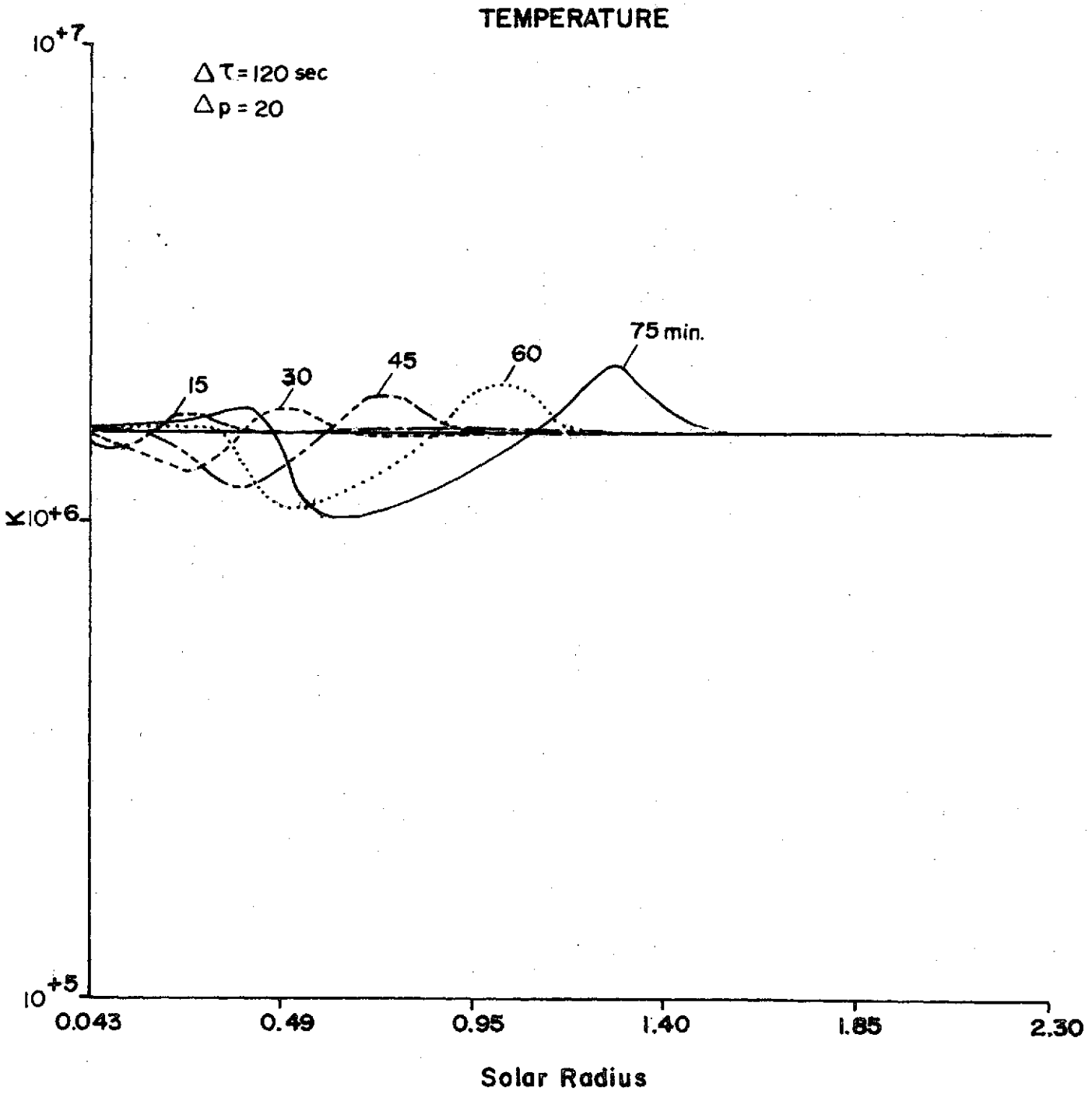
TEMPERATURE
10^{+7}
$\Delta\tau$ = 120 sec
Δp = 20
15
30
45
60
75 min.
$\times 10^{+6}$
10^{+5}
0.043
0.49
0.95
1.40
1.85
2.30
Solar Radius

FIG. 3-b

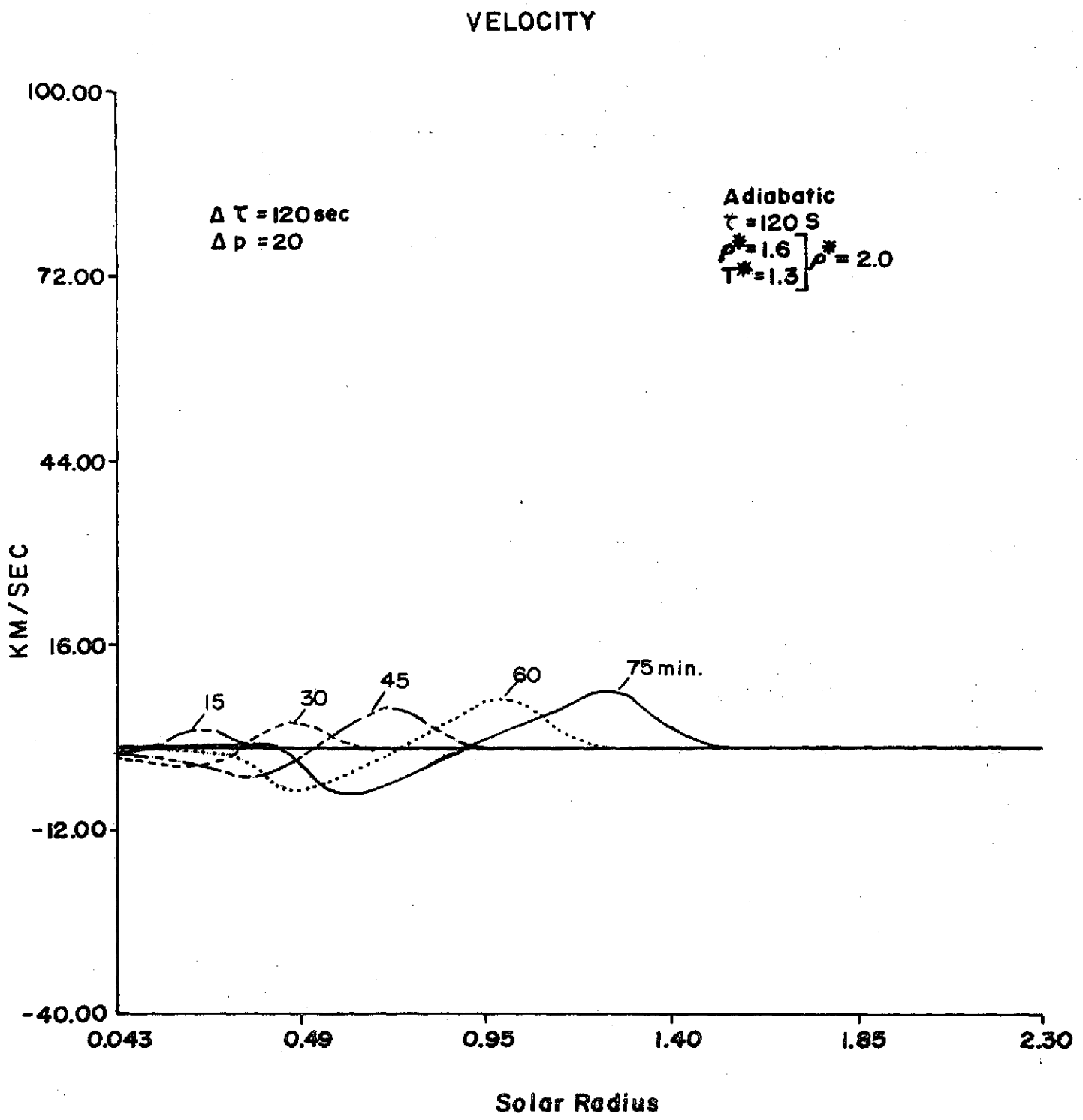
VELOCITY
100.00
72.00
44.00
16.00
-12.00
-40.00
KM/SEC
Δ τ = 120 sec
Δ p = 20
Adiabatic
τ = 120 S
ρ* = 1.6
T* = 1.3
ρ* = 2.0
15
30
45
60
75 min.
0.043
0.49
0.95
1.40
1.85
2.30
Solar Radius

FIG. 3-c

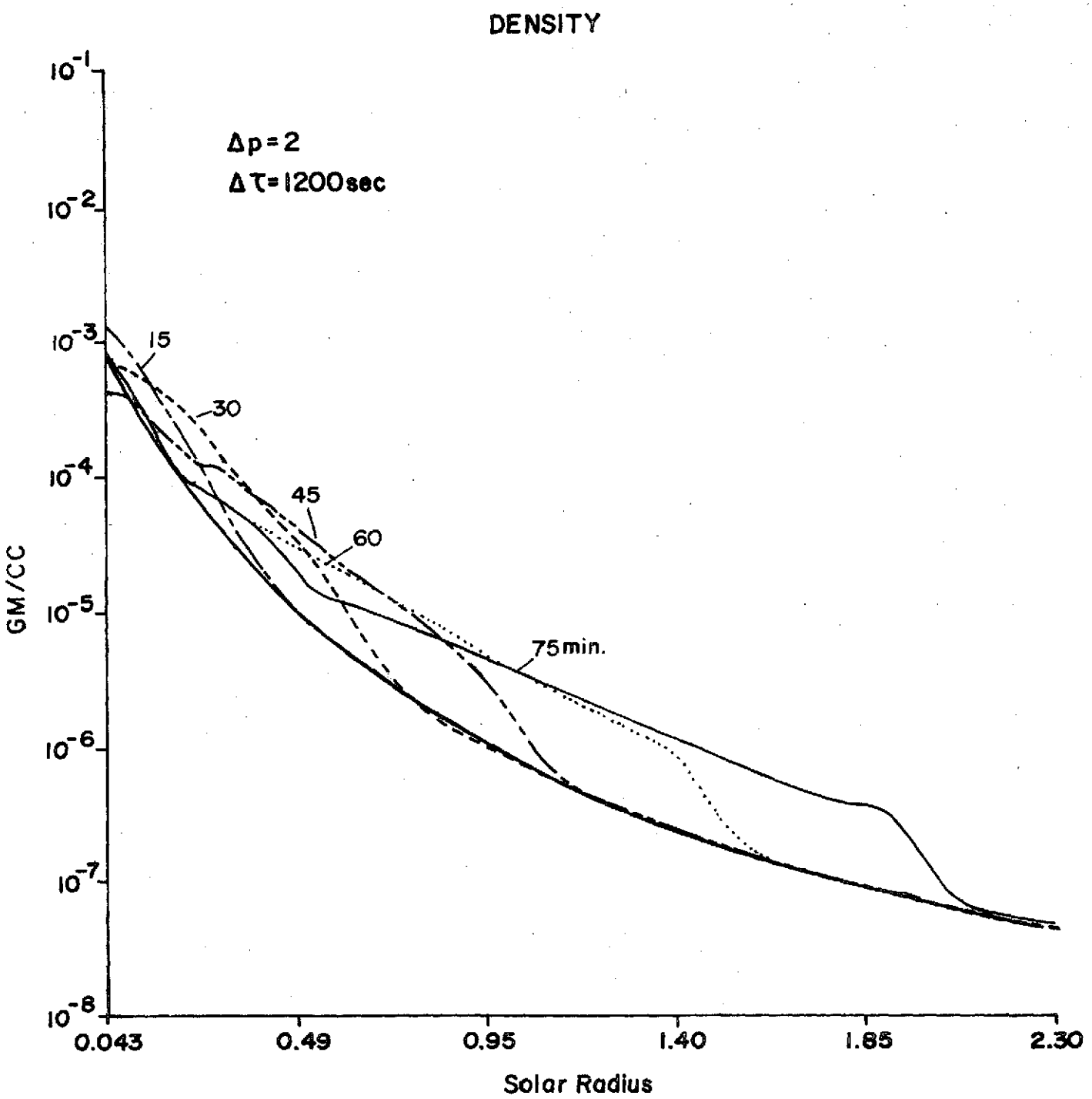
DENSITY
Δp=2
Δτ=1200sec
15
30
45
60
75min.
GM/CC
10^-1
10^-2
10^-3
10^-4
10^-5
10^-6
10^-7
10^-8
0.043
0.49
0.95
1.40
1.85
2.30
Solar Radius

FIG. 4-a

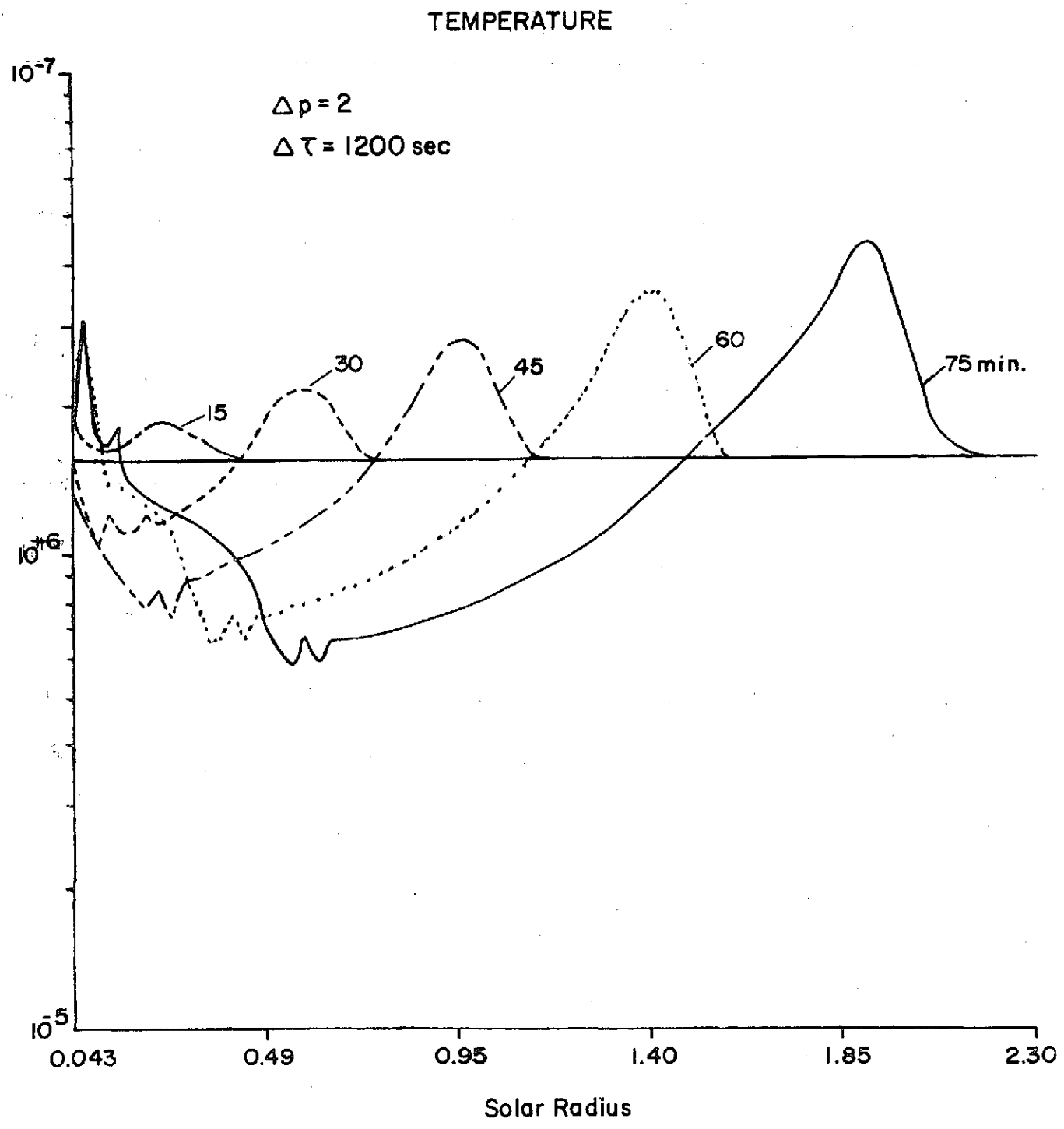
TEMPERATURE
10^{-7}
$\Delta p = 2$
$\Delta \tau = 1200$ sec
15
30
45
60
75 min.
10^{+6}
10^{5}
0.043
0.49
0.95
1.40
1.85
2.30
Solar Radius

FIG. 4-b

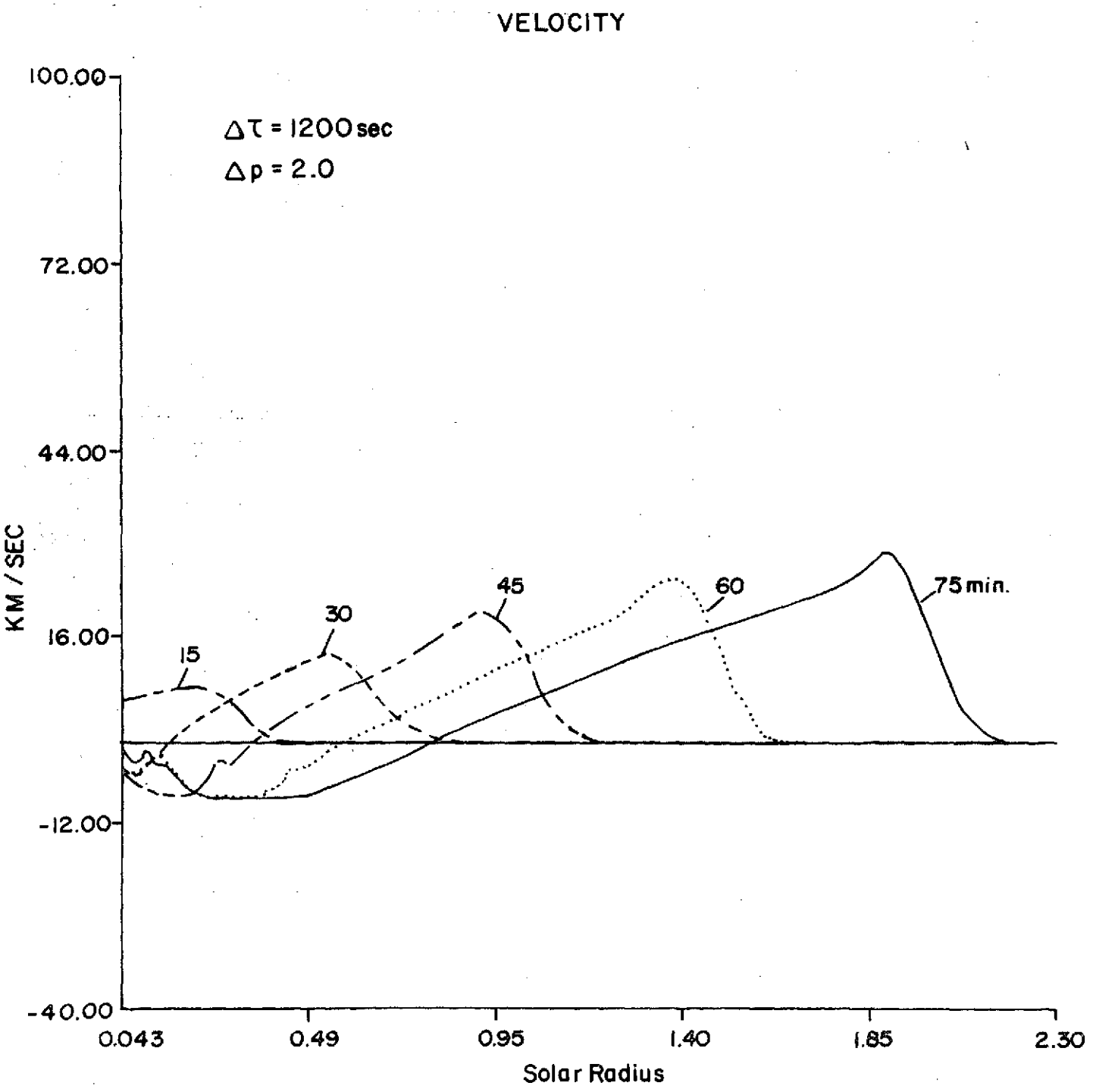
VELOCITY
100.00
72.00
44.00
16.00
-12.00
-40.00
KM / SEC
ΔT = 1200 sec
Δp = 2.0
15
30
45
60
75 min.
0.043
0.49
0.95
1.40
1.85
2.30
Solar Radius

FIG. 4-c

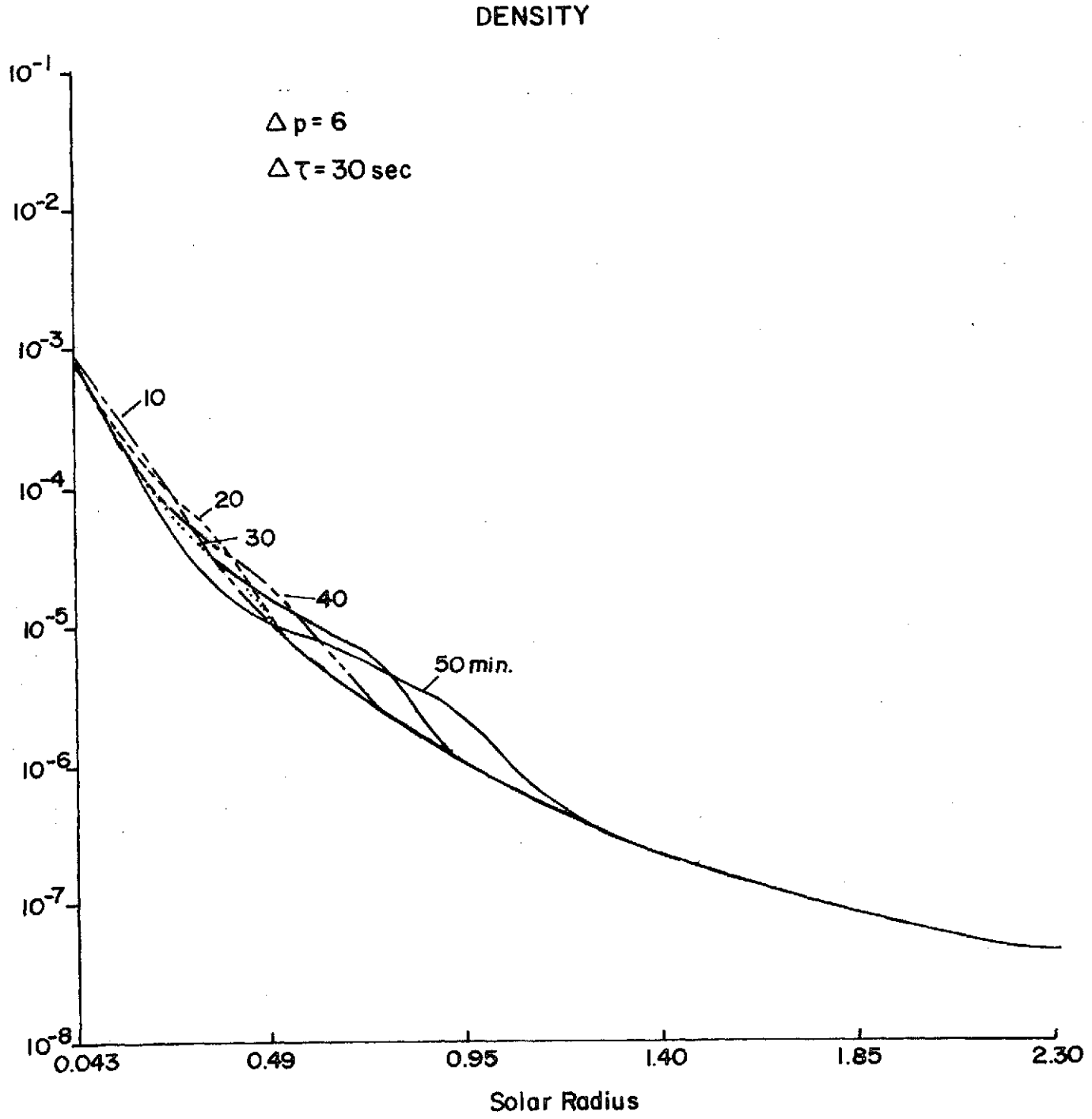
DENSITY
Δ p = 6
Δ τ = 30 sec
10
20
30
40
50 min.
10^-1
10^-2
10^-3
10^-4
10^-5
10^-6
10^-7
10^-8
0.043
0.49
0.95
1.40
1.85
2.30
Solar Radius

FIG. 5-a

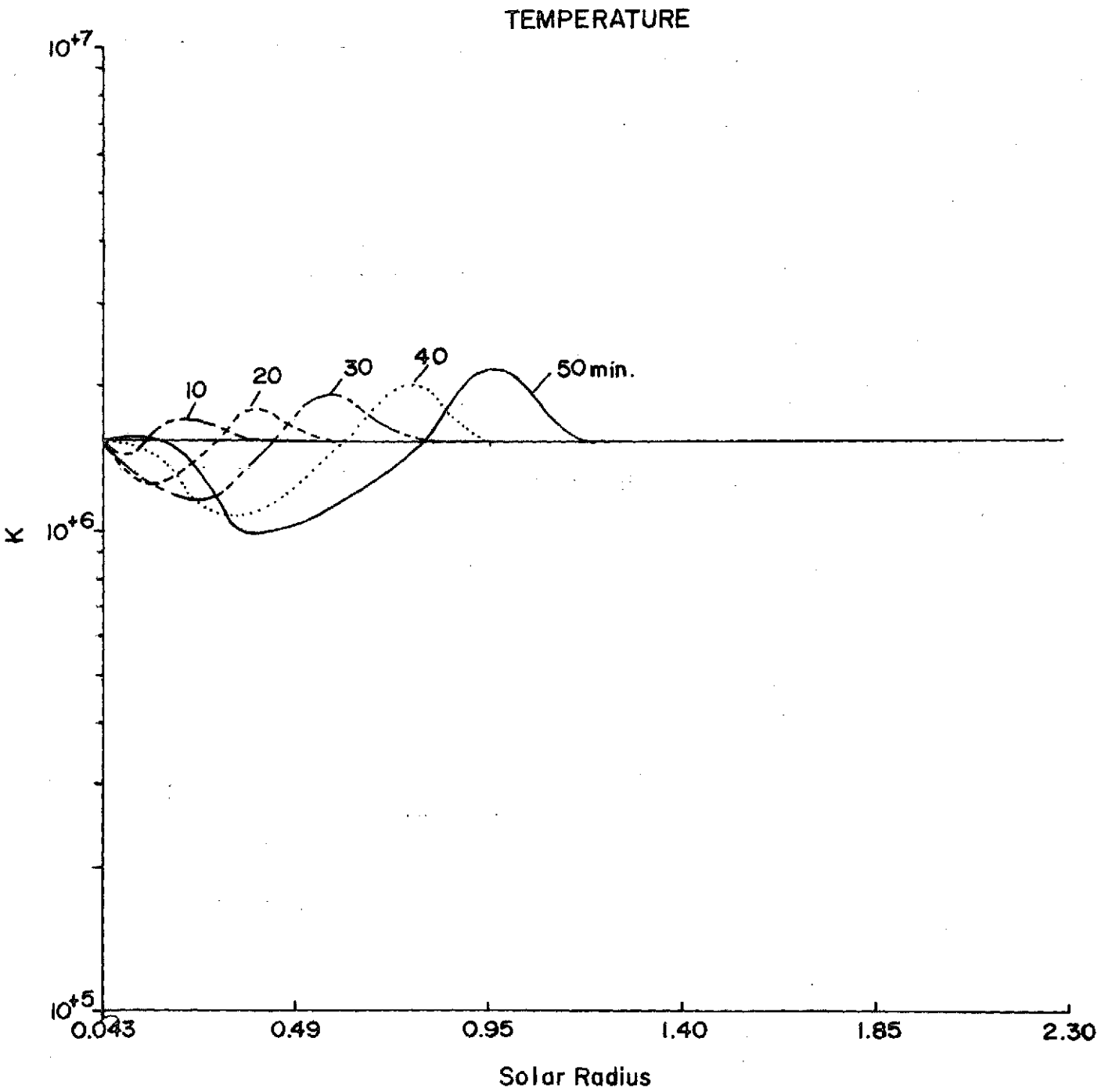
TEMPERATURE
10+7
10+6
10+5
K
10
20
30
40
50 min.
0.043
0.49
0.95
1.40
1.85
2.30
Solar Radius

FIG. 5-b

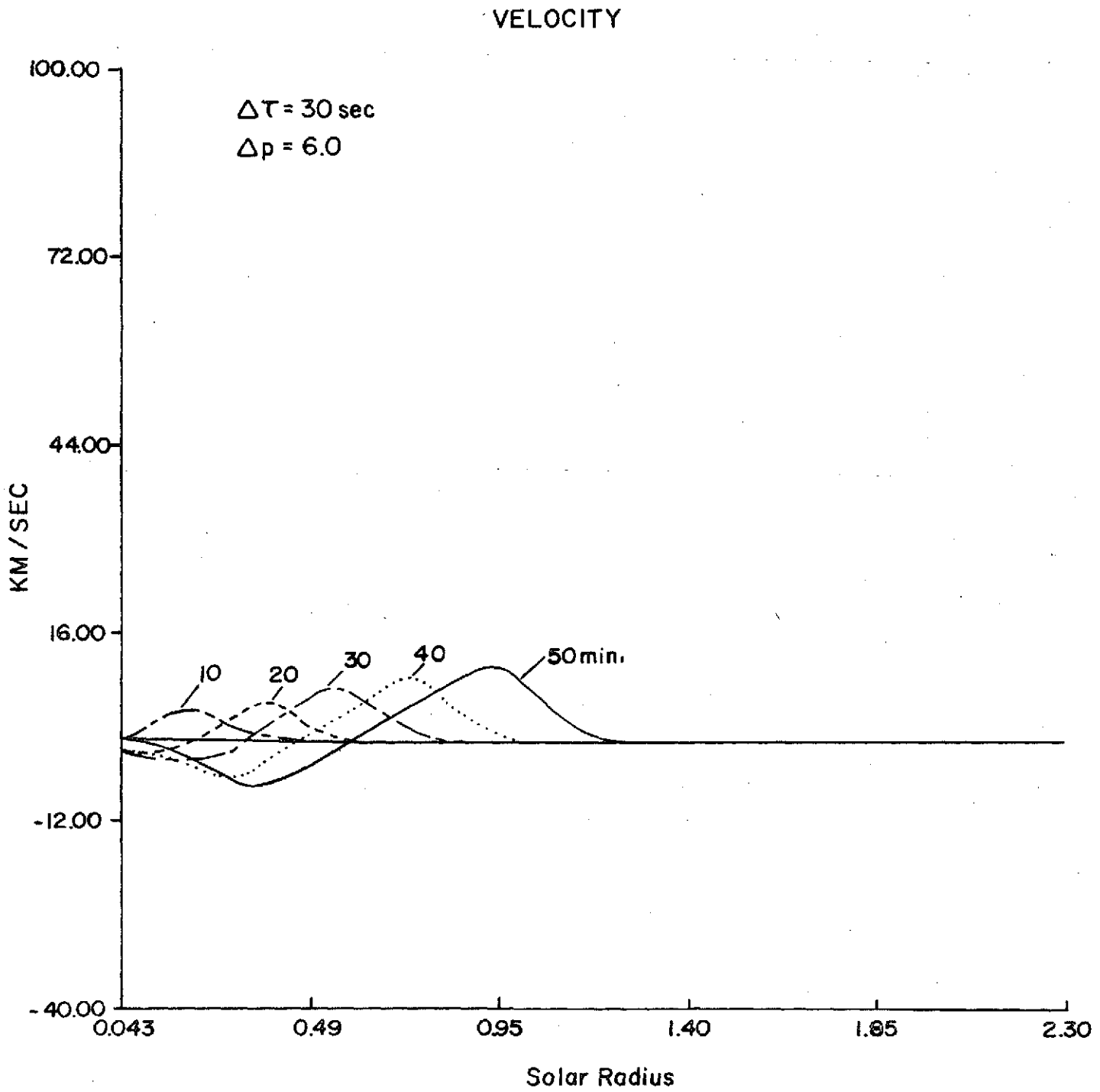
VELOCITY
ΔT = 30 sec
Δp = 6.0
100.00
72.00
44.00
16.00
-12.00
-40.00
KM / SEC
10
20
30
40
50 min.
0.043
0.49
0.95
1.40
1.85
2.30
Solar Radius

FIG.-5-c

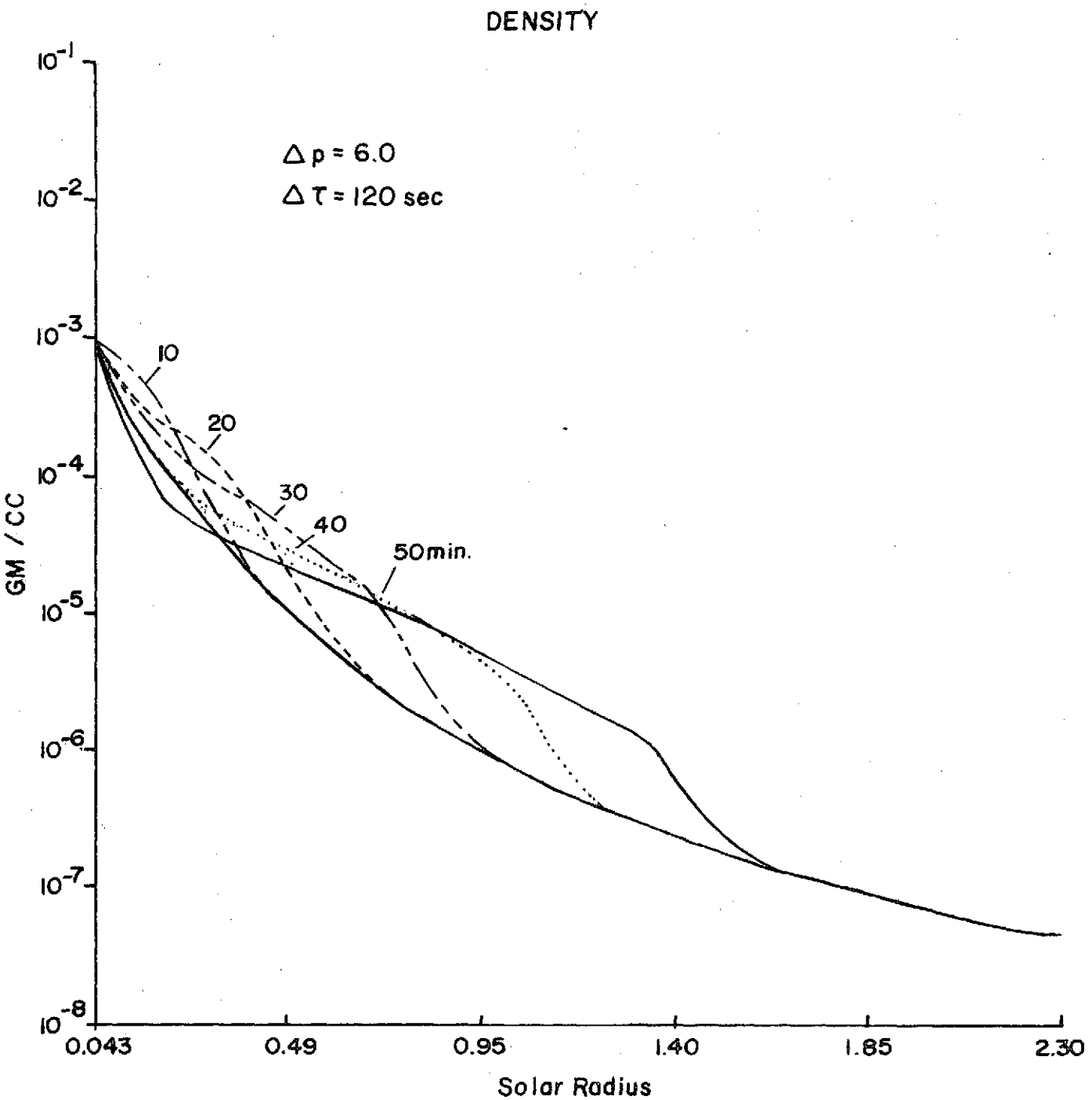
DENSITY
Δp = 6.0
Δτ = 120 sec
10
20
30
40
50min.
GM / CC
10^-1
10^-2
10^-3
10^-4
10^-5
10^-6
10^-7
10^-8
0.043
0.49
0.95
1.40
1.85
2.30
Solar Radius

FIG.6-a

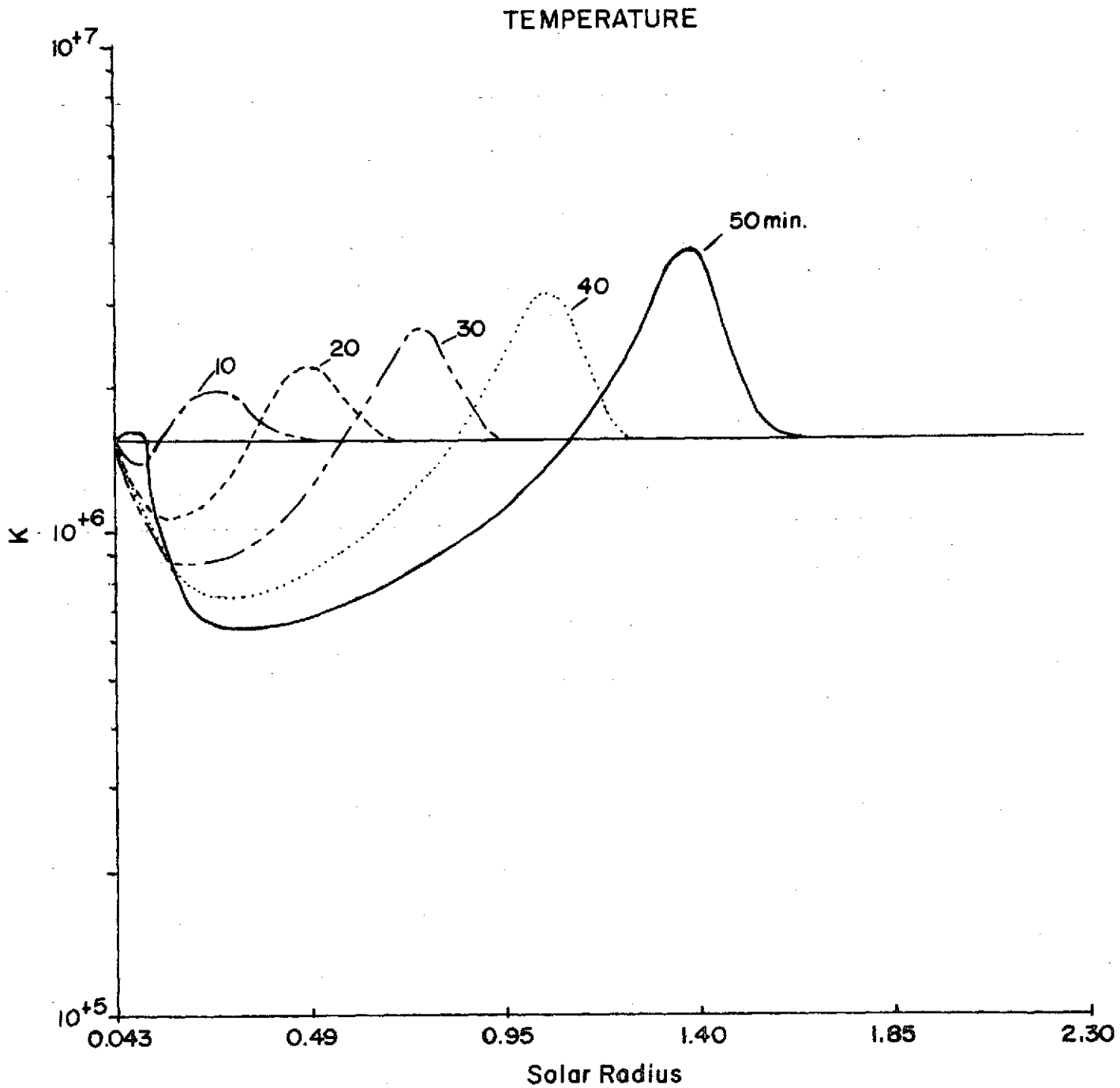
TEMPERATURE
10^{+7}
$K \cdot 10^{+6}$
10^{+5}
10
20
30
40
50 min.
0.043
0.49
0.95
1.40
1.85
2.30
Solar Radius

FIG. 6-b

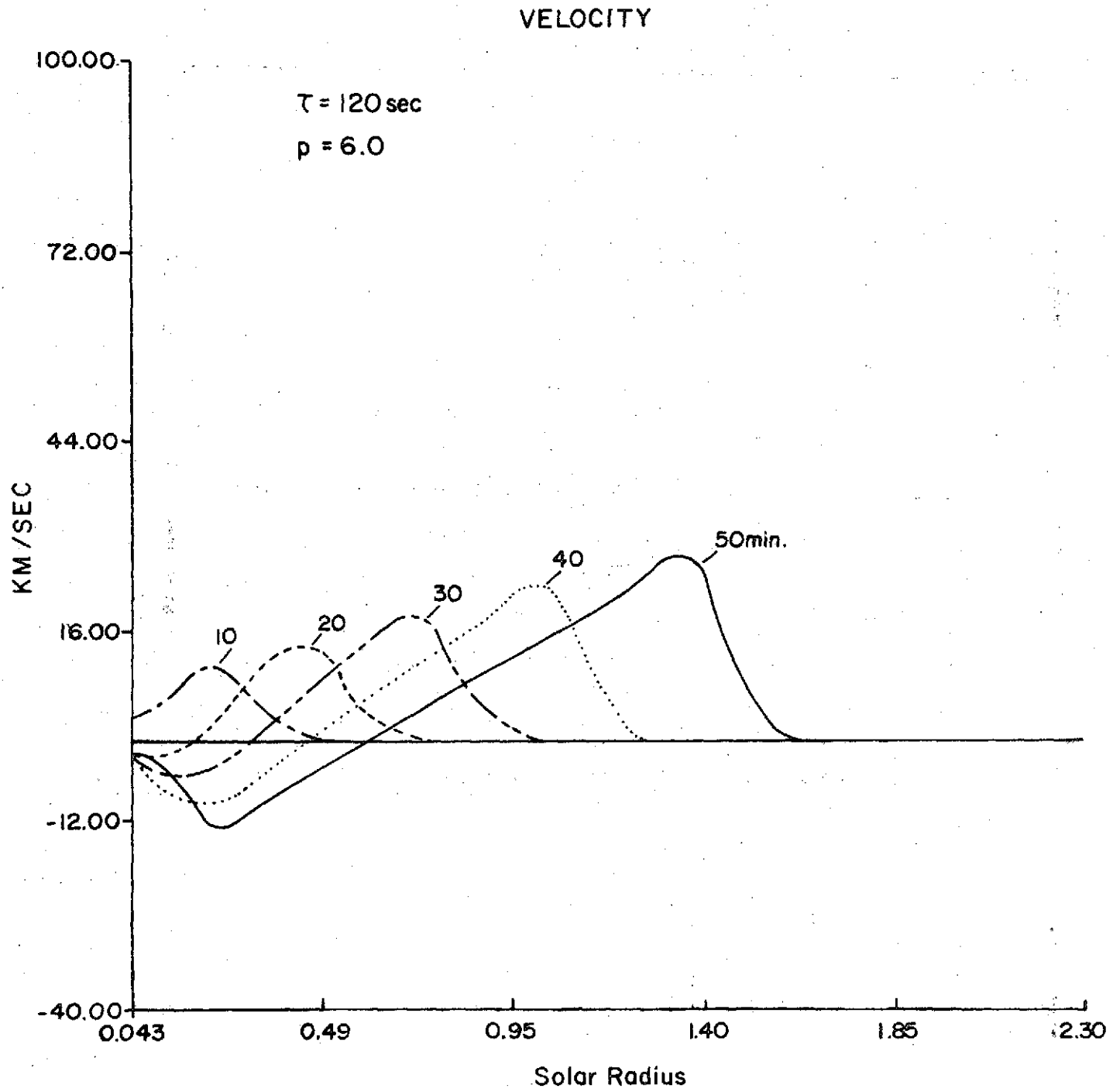
VELOCITY
τ = 120 sec
p = 6.0
100.00
72.00
44.00
16.00
-12.00
-40.00
KM/SEC
10
20
30
40
50min.
0.043
0.49
0.95
1.40
1.85
2.30
Solar Radius

FIG. 6-c

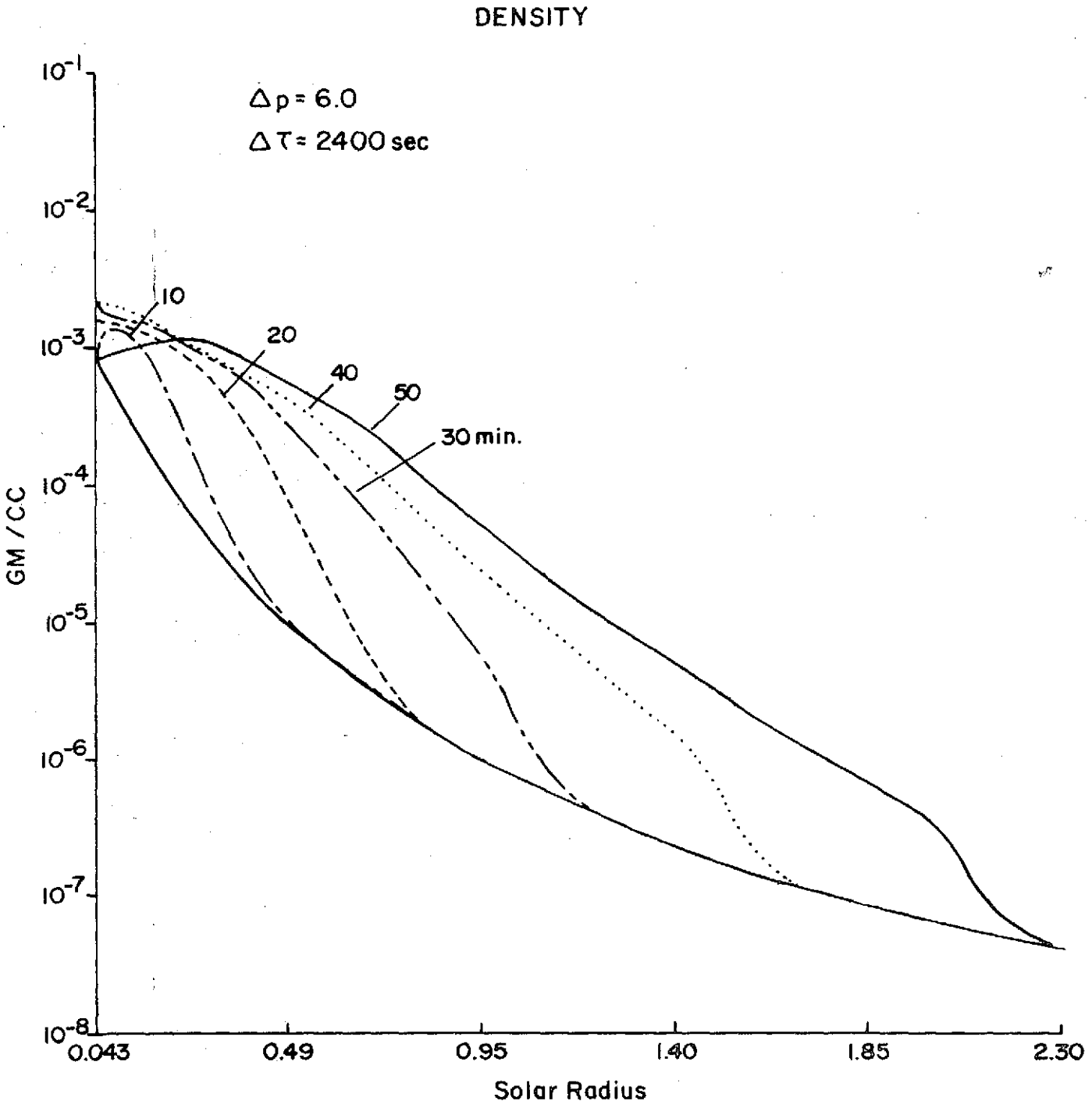
DENSITY
Δp = 6.0
Δτ = 2400 sec
10
20
40
50
30 min.
GM / CC
10^-1
10^-2
10^-3
10^-4
10^-5
10^-6
10^-7
10^-8
0.043
0.49
0.95
1.40
1.85
2.30
Solar Radius

FIG. 7-a

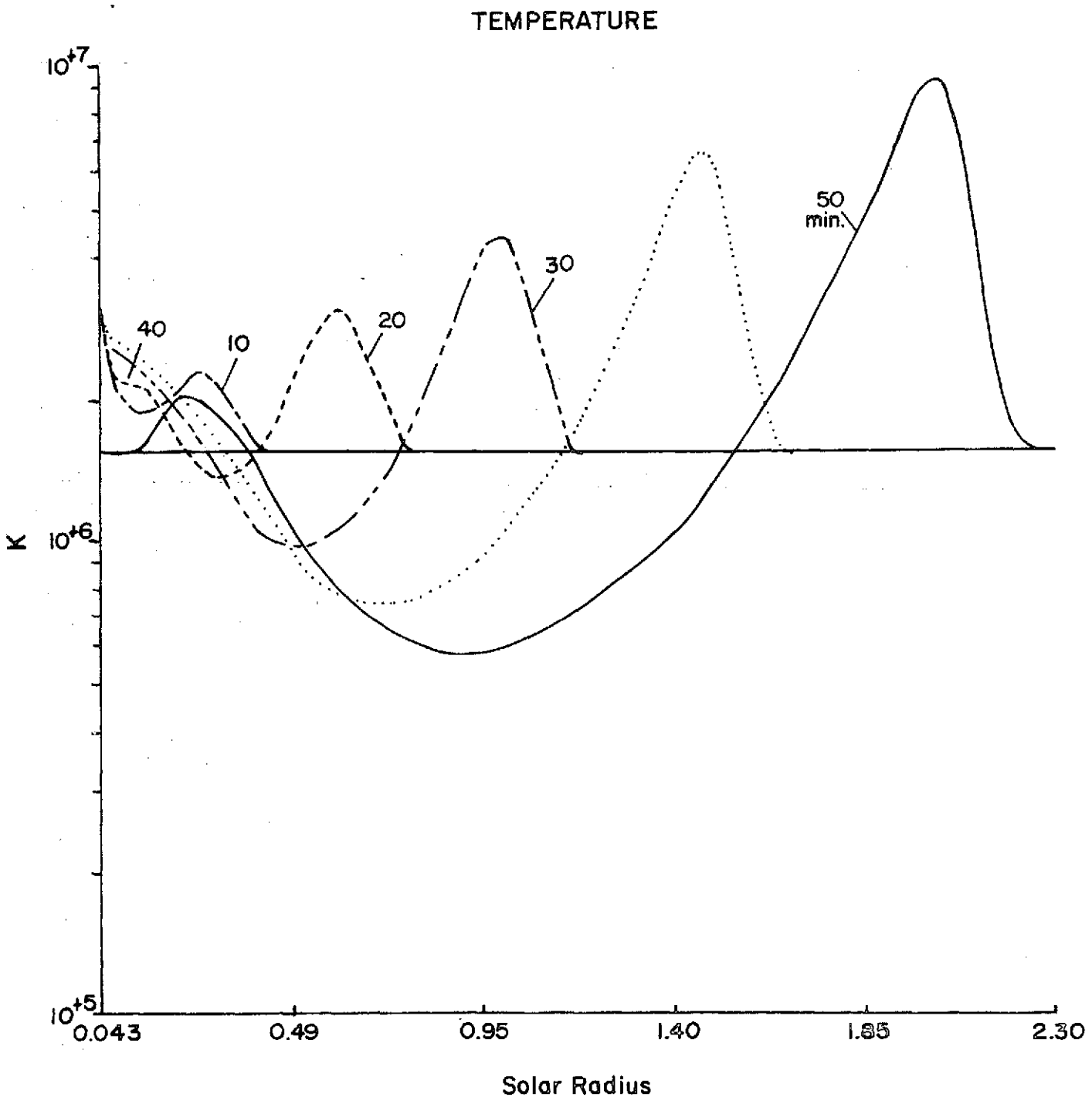
TEMPERATURE
10^{+7}
10^{+6}
10^{+5}
K
40
10
20
30
50
min.
0.043
0.49
0.95
1.40
1.85
2.30
Solar Radius

FIG. 7-b

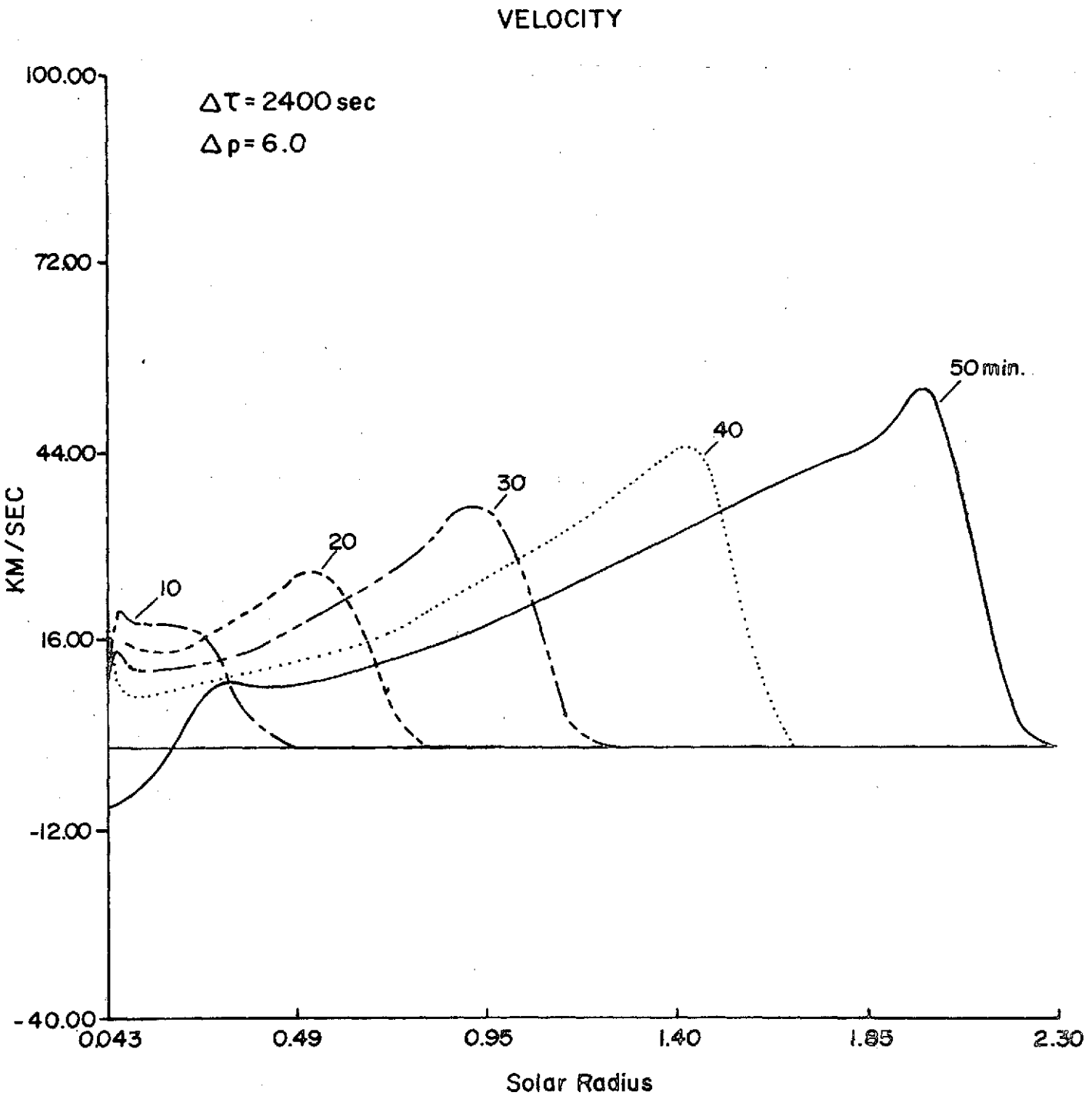
VELOCITY
ΔT = 2400 sec
Δp = 6.0
100.00
72.00
44.00
16.00
-12.00
-40.00
KM/SEC
10
20
30
40
50 min.
0.043
0.49
0.95
1.40
1.85
2.30
Solar Radius

FIG. 7-c

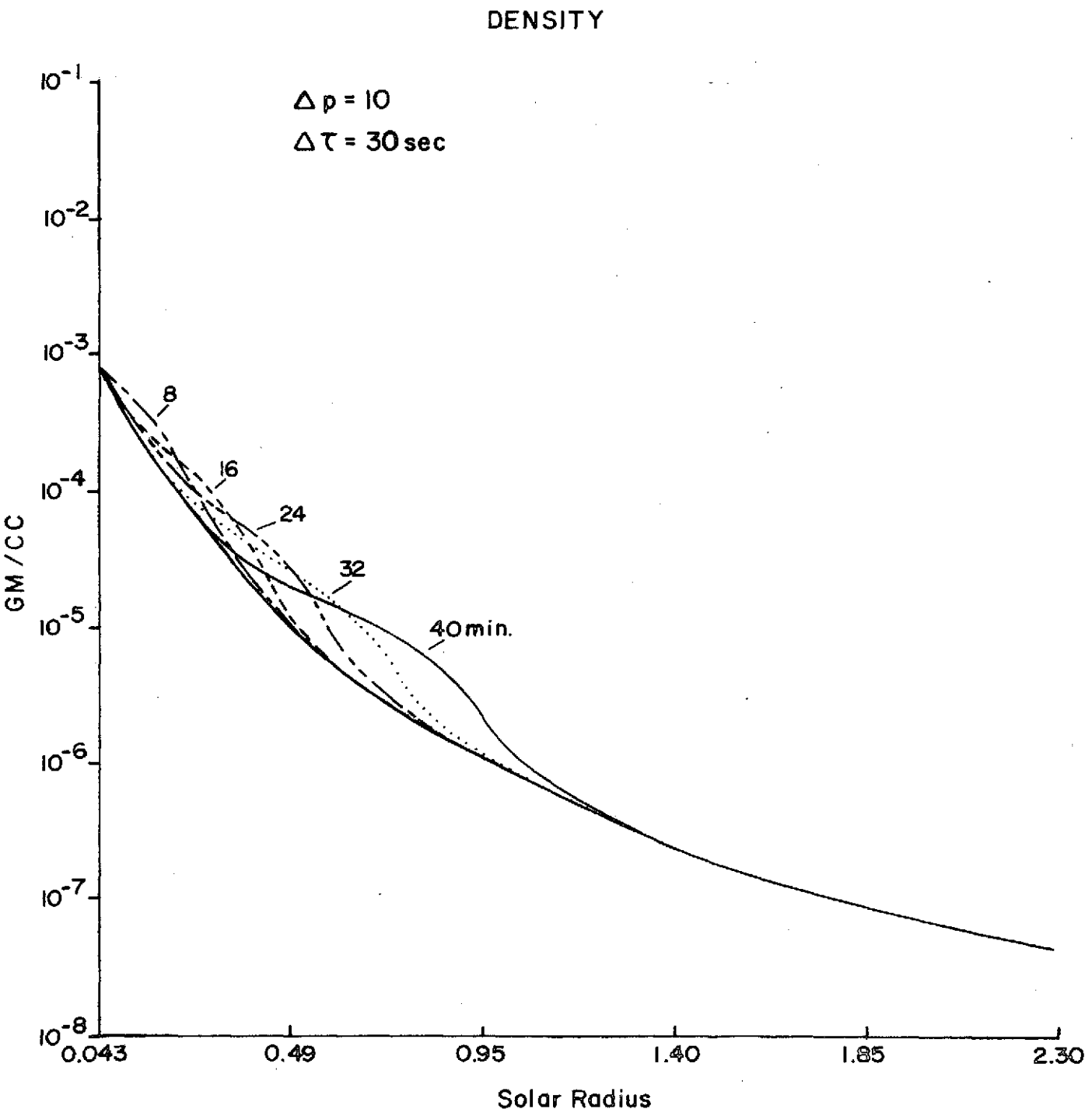
DENSITY
Δp = 10
Δτ = 30 sec
10^-1
10^-2
10^-3
10^-4
10^-5
10^-6
10^-7
10^-8
GM/CC
8
16
24
32
40 min.
0.043
0.49
0.95
1.40
1.85
2.30
Solar Radius

FIG. 8-a

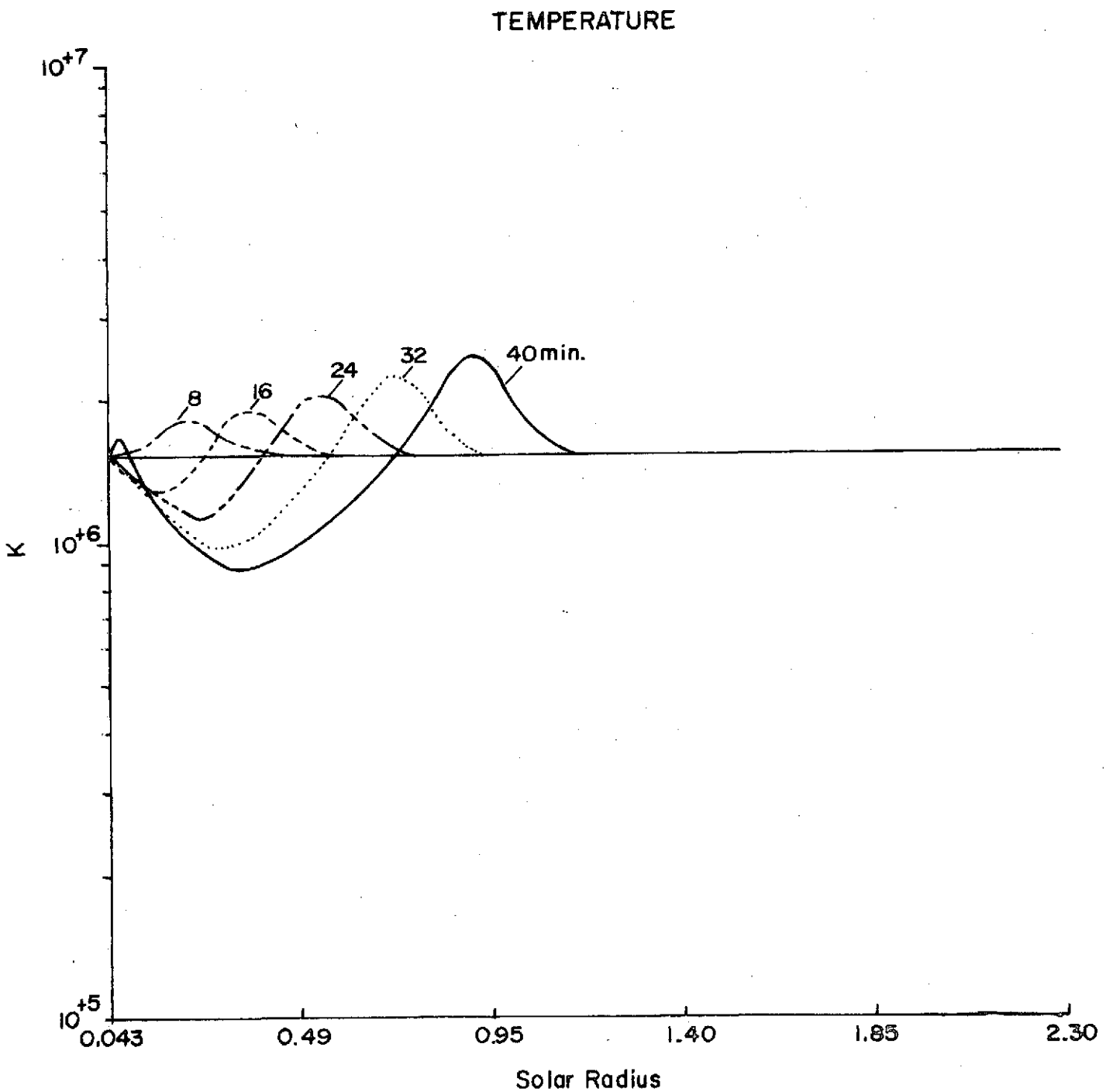
TEMPERATURE
10^{+7}
10^{+6}
10^{+5}
K
8
16
24
32
40min.
0.043
0.49
0.95
1.40
1.85
2.30
Solar Radius

FIG. 8-b

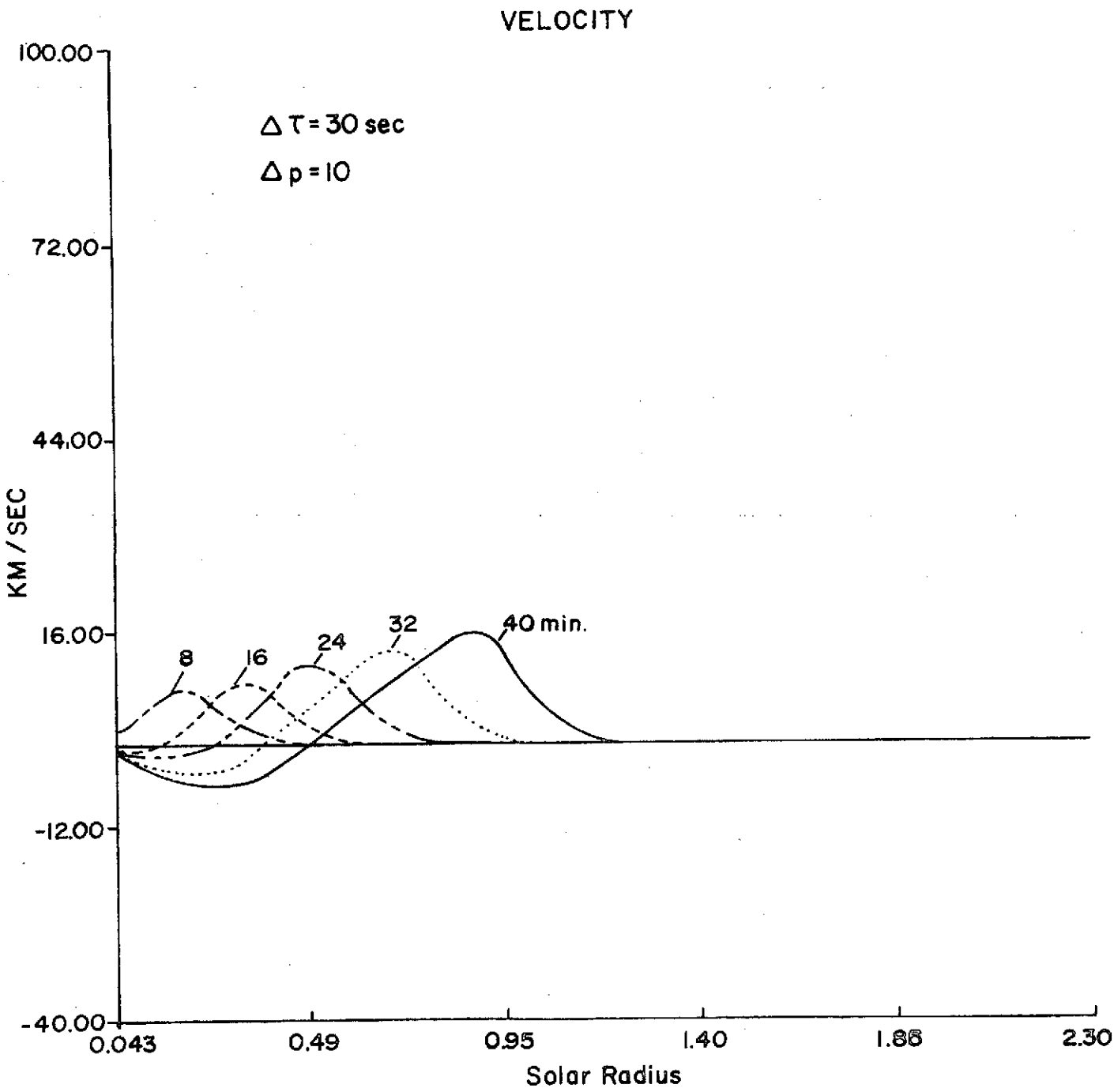
VELOCITY
100.00
72.00
44.00
16.00
-12.00
-40.00
KM / SEC
Δ T = 30 sec
Δ p = 10
8
16
24
32
40 min.
0.043
0.49
0.95
1.40
1.88
2.30
Solar Radius

FIG.8-c

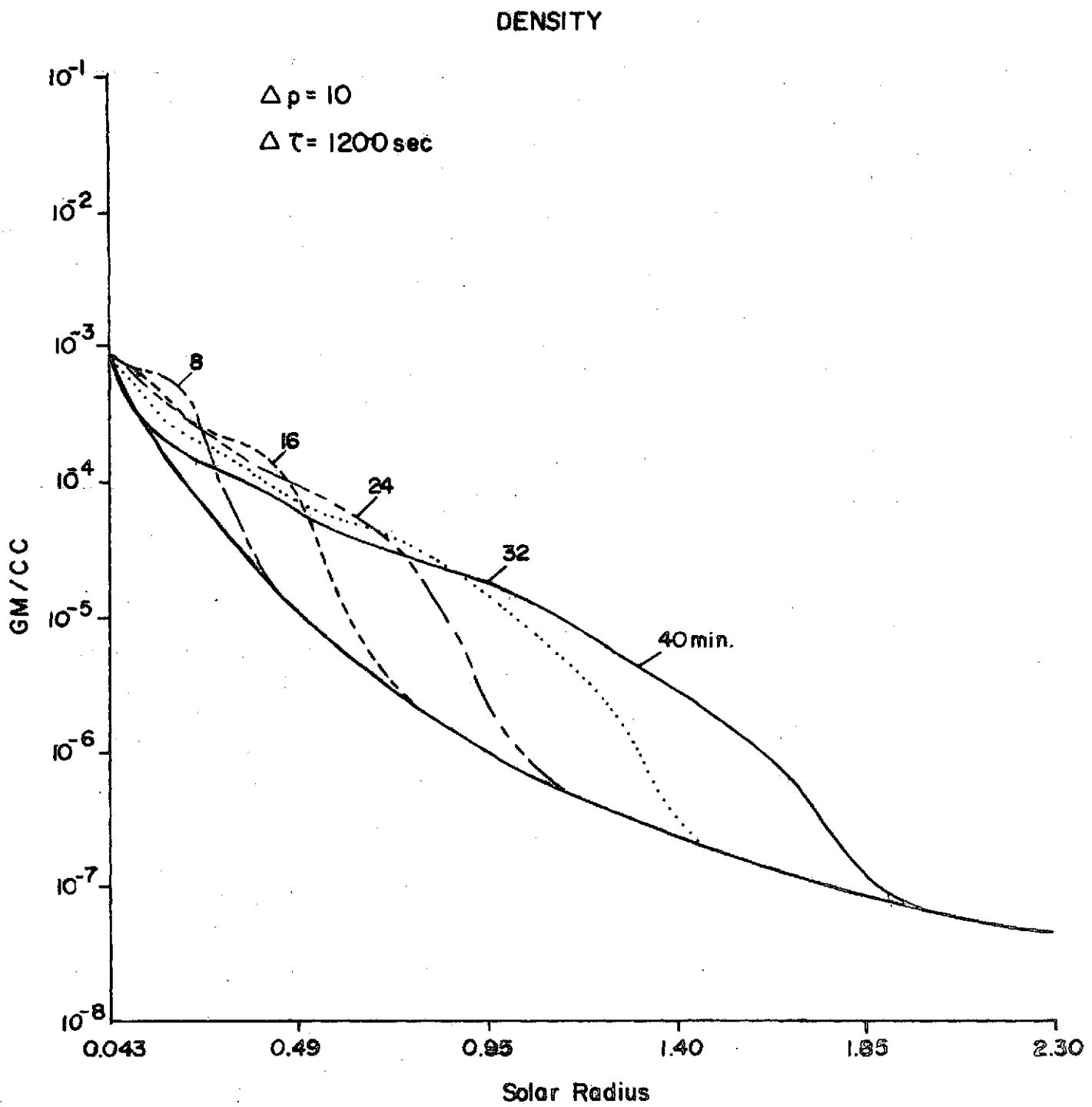
DENSITY
Δ p = 10
Δ τ = 1200 sec
10^-1
10^-2
10^-3
10^-4
10^-5
10^-6
10^-7
10^-8
GM / CC
8
16
24
32
40 min.
0.043
0.49
0.93
1.40
1.85
2.30
Solar Radius

FIG. 9-a

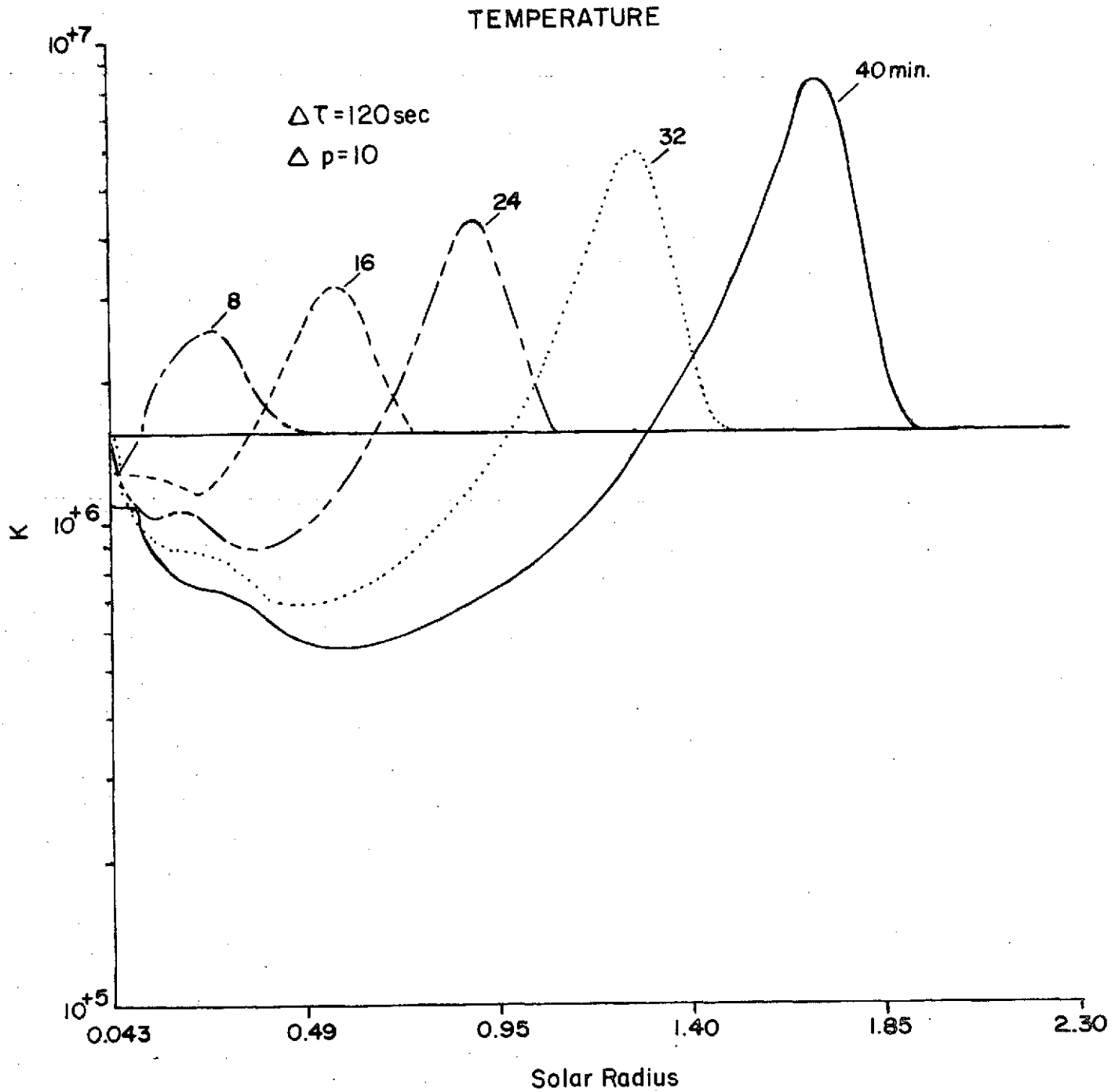
TEMPERATURE
10^{+7}
10^{+6}
10^{+5}
K
ΔT = 120 sec
Δ p = 10
8
16
24
32
40 min.
0.043
0.49
0.95
1.40
1.85
2.30
Solar Radius

FIG. 9-b

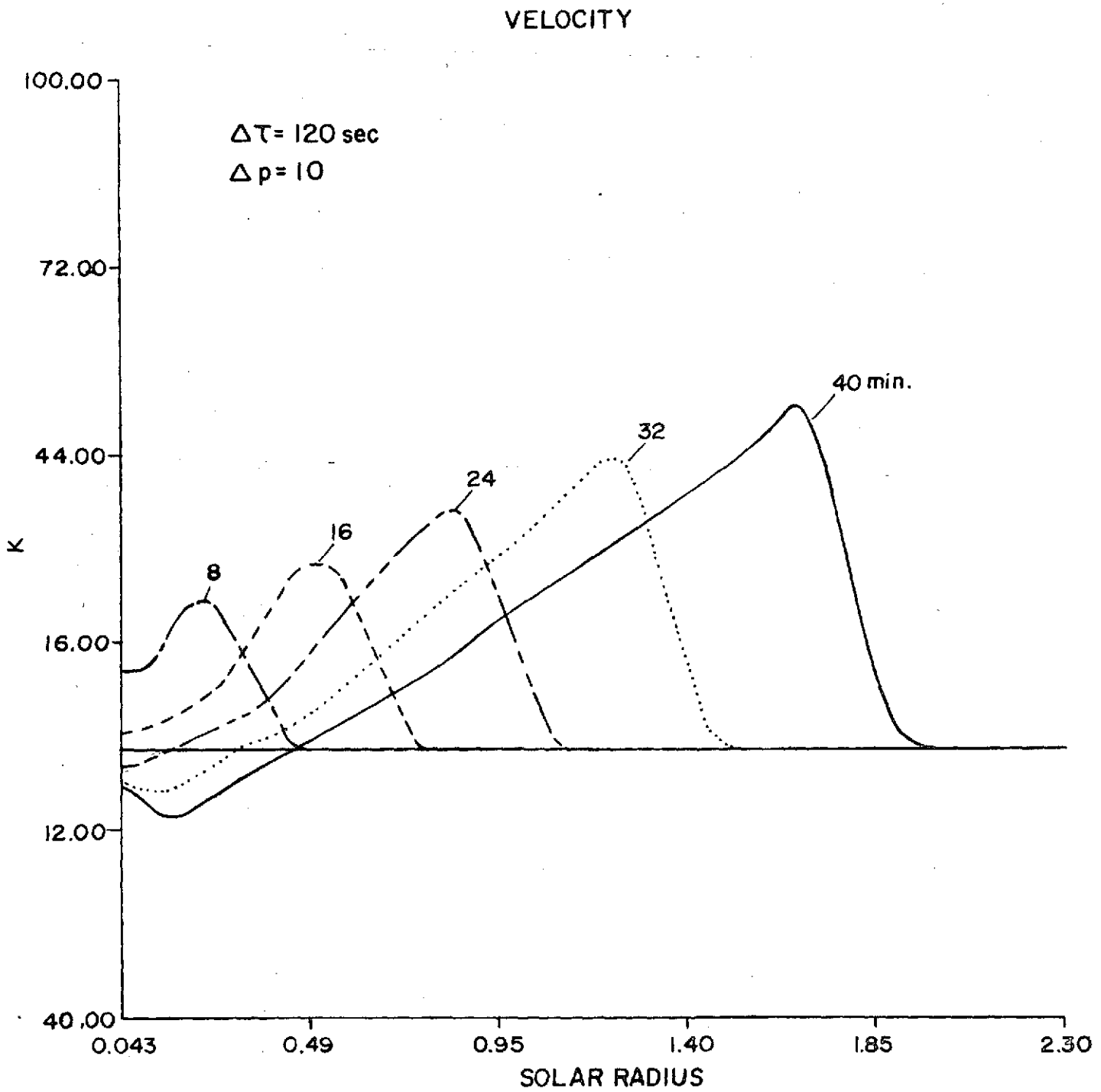
VELOCITY
100.00
72.00
44.00
16.00
12.00
40.00
K
ΔT= 120 sec
Δ p= 10
8
16
24
32
40 min.
0.043
0.49
0.95
1.40
1.85
2.30
SOLAR RADIUS

FIG. 9-c

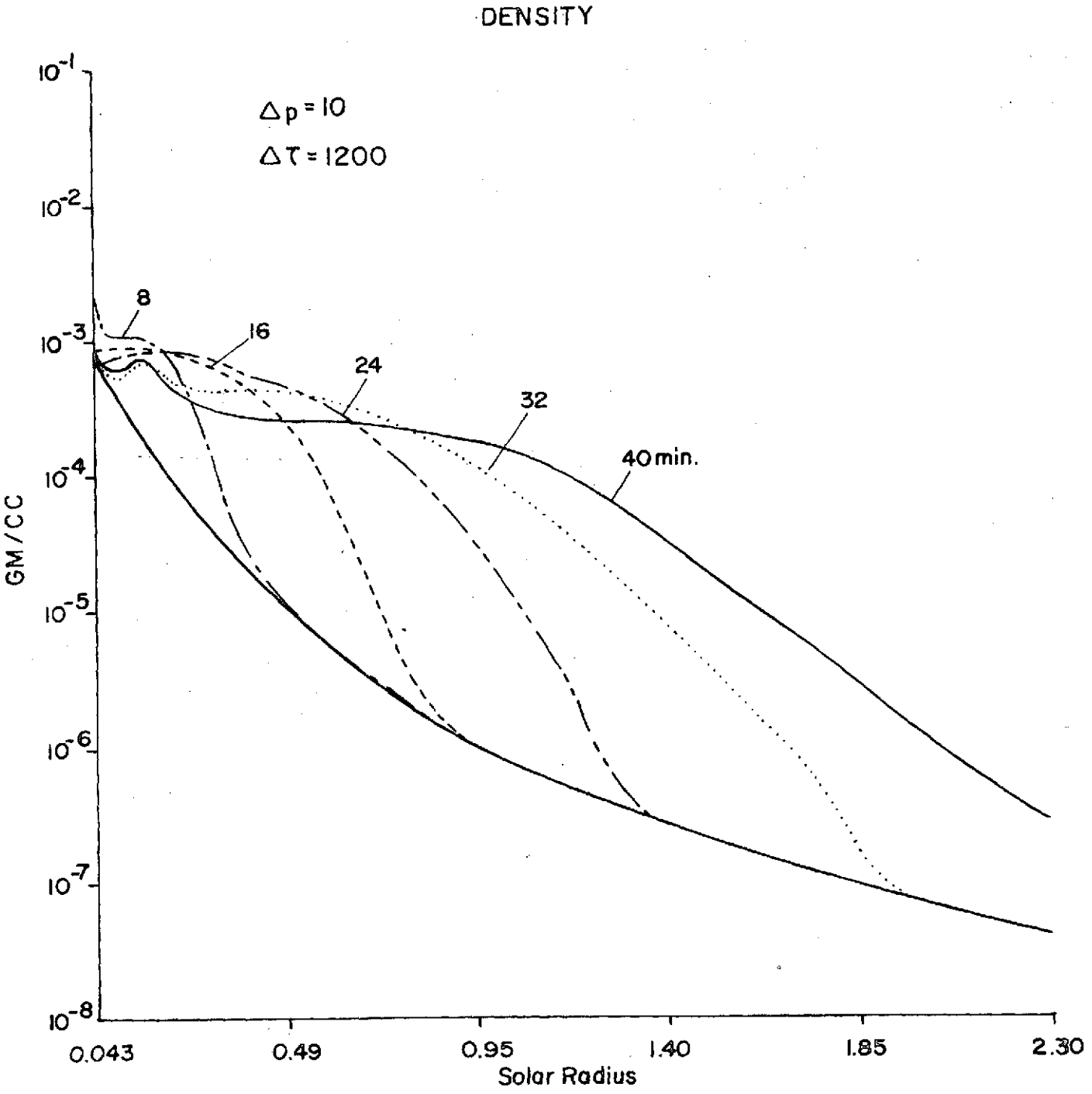
DENSITY
Δp = 10
Δτ = 1200
8
16
24
32
40 min.
GM/CC
10^-1
10^-2
10^-3
10^-4
10^-5
10^-6
10^-7
10^-8
0.043
0.49
0.95
1.40
1.85
2.30
Solar Radius

FIG. 10-a

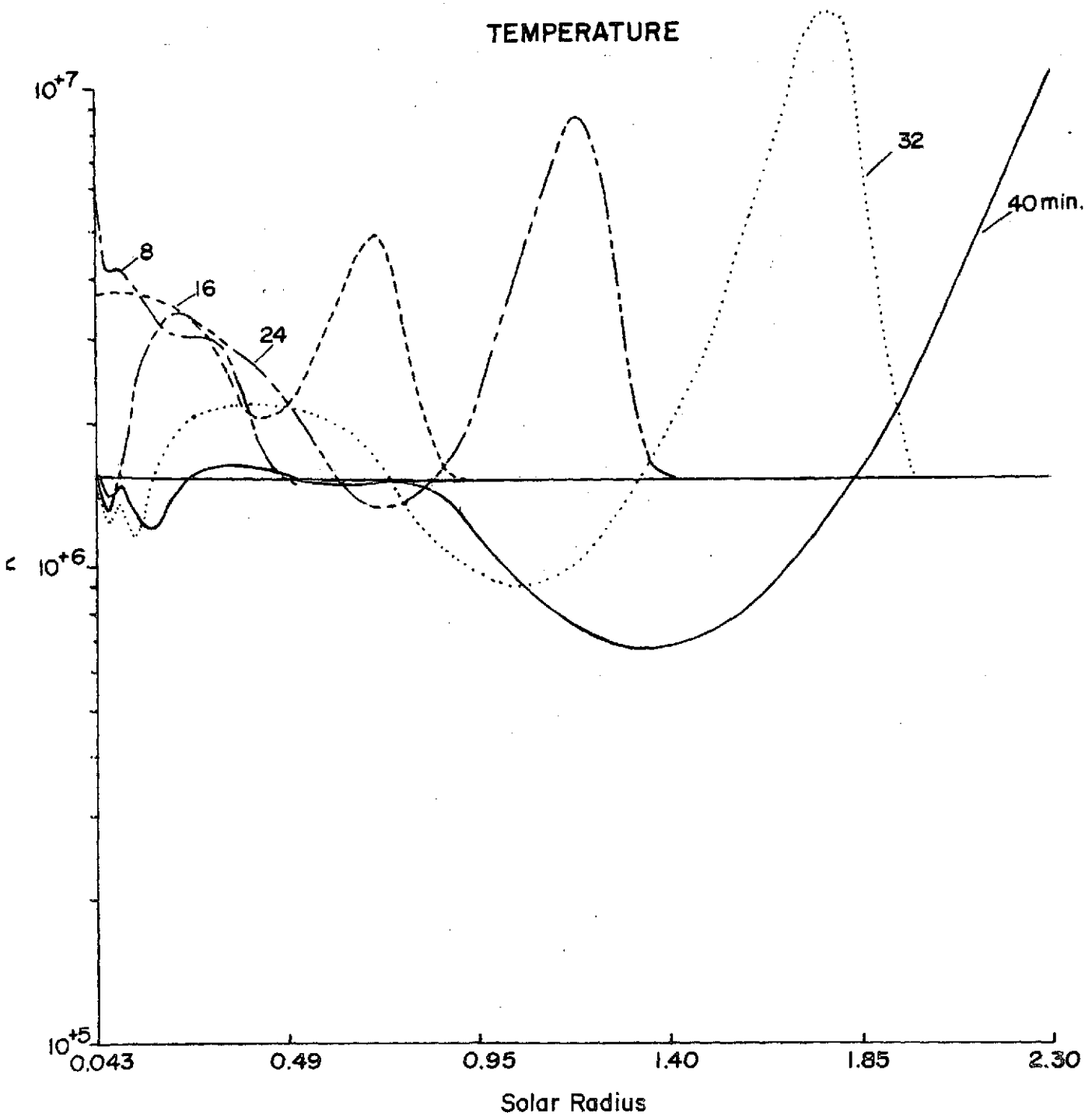
TEMPERATURE
10^{+7}
10^{+6}
10^{+5}
8
16
24
32
40 min.
0.043
0.49
0.95
1.40
1.85
2.30
Solar Radius

FIG. 10-b

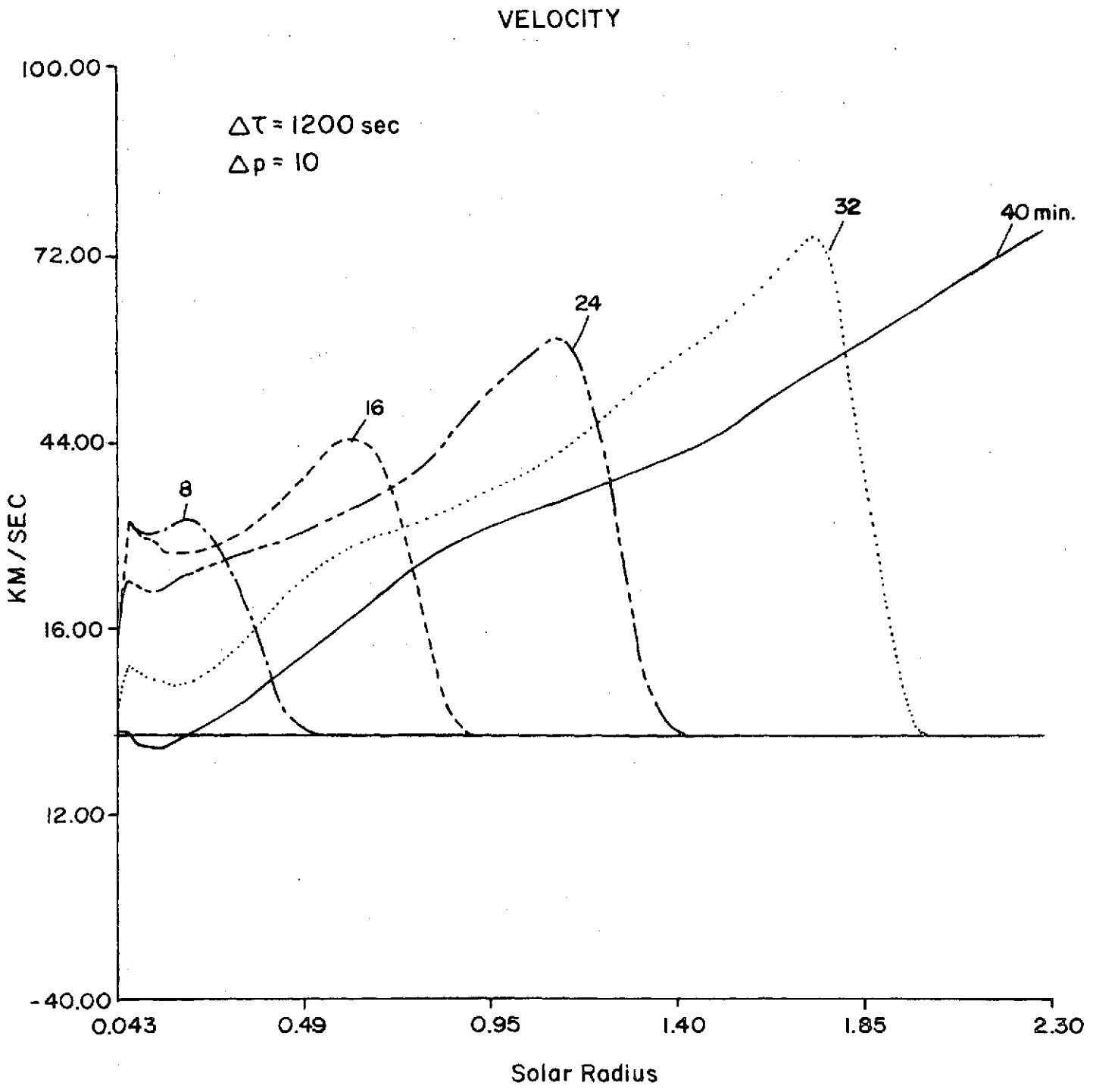
VELOCITY
100.00
72.00
44.00
16.00
12.00
-40.00
Δτ = 1200 sec
Δp = 10
8
16
24
32
40 min.
KM/SEC
0.043
0.49
0.95
1.40
1.85
2.30
Solar Radius

FIG. 10-c

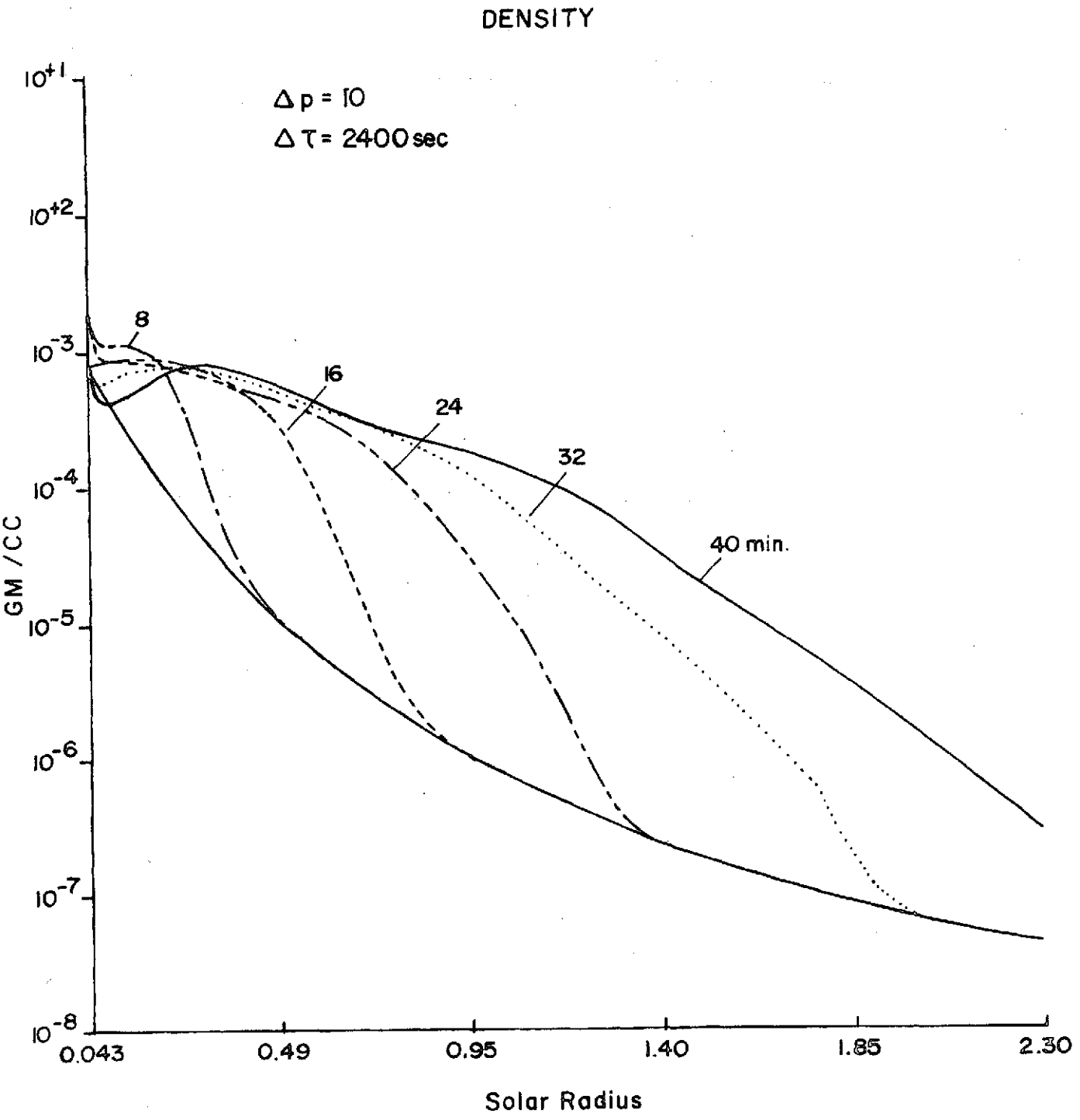
DENSITY
Δ p = 10
Δ τ = 2400 sec
10+1
10+2
10-3
10-4
10-5
10-6
10-7
10-8
GM / CC
8
16
24
32
40 min.
0.043
0.49
0.95
1.40
1.85
2.30
Solar Radius

FIG. II-a

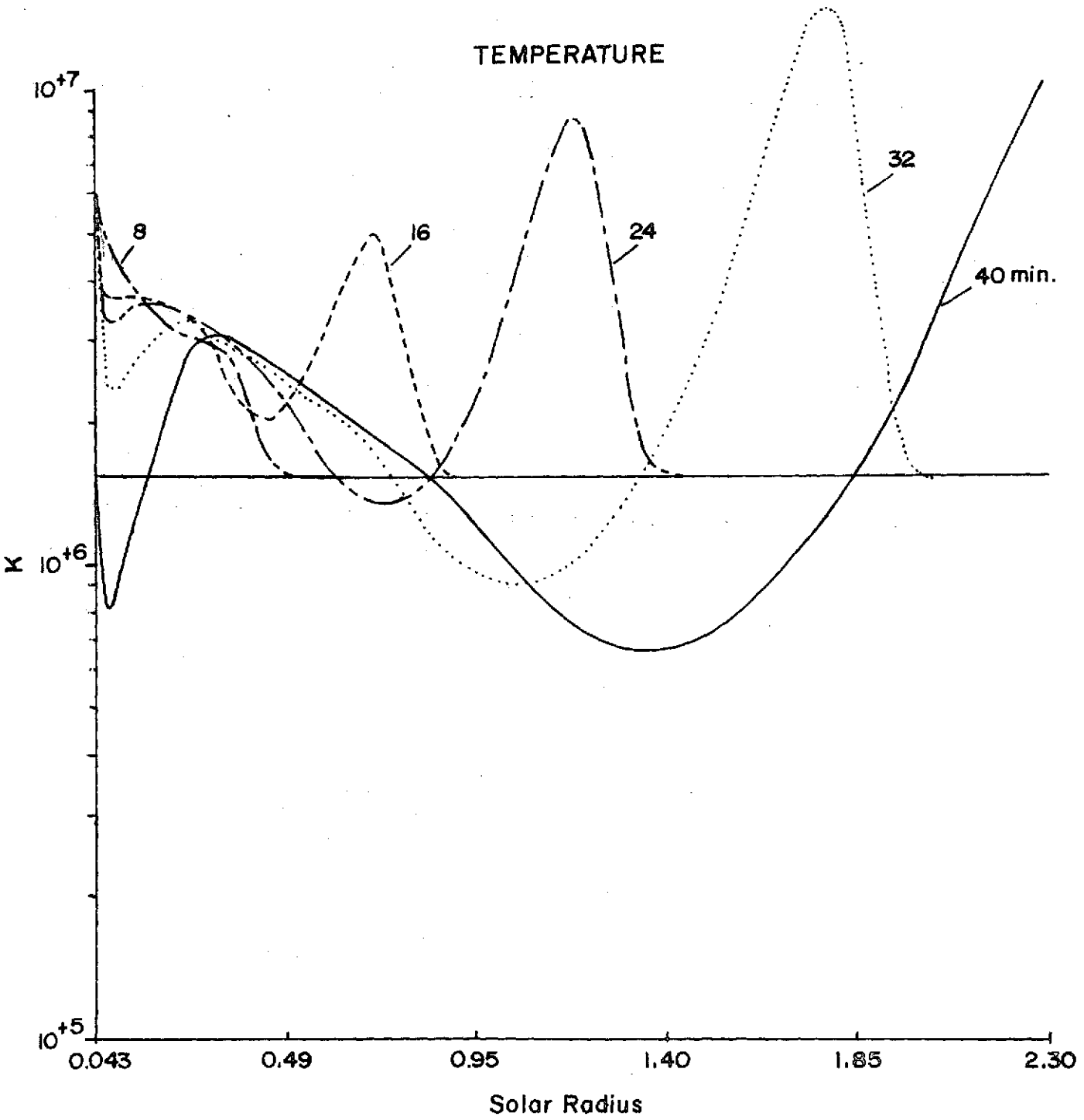
TEMPERATURE
10^{+7}
10^{+6}
10^{+5}
K
8
16
24
32
40 min.
0.043
0.49
0.95
1.40
1.85
2.30
Solar Radius

FIG. 11-b

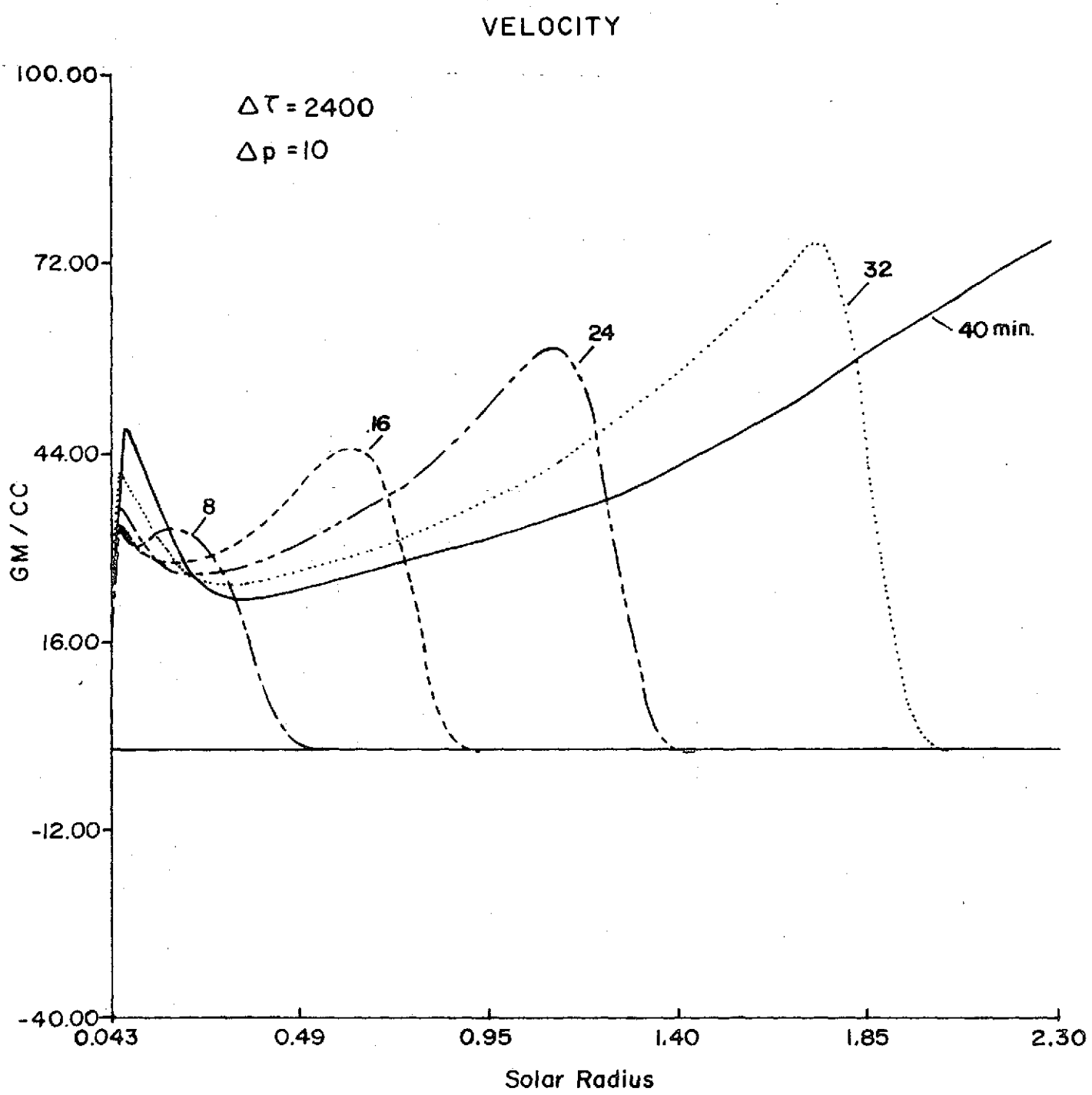
VELOCITY
100.00
72.00
44.00
16.00
-12.00
-40.00
ΔT = 2400
Δp = 10
8
16
24
32
40 min.
GM / CC
0.043
0.49
0.95
1.40
1.85
2.30
Solar Radius

FIG. 11-c

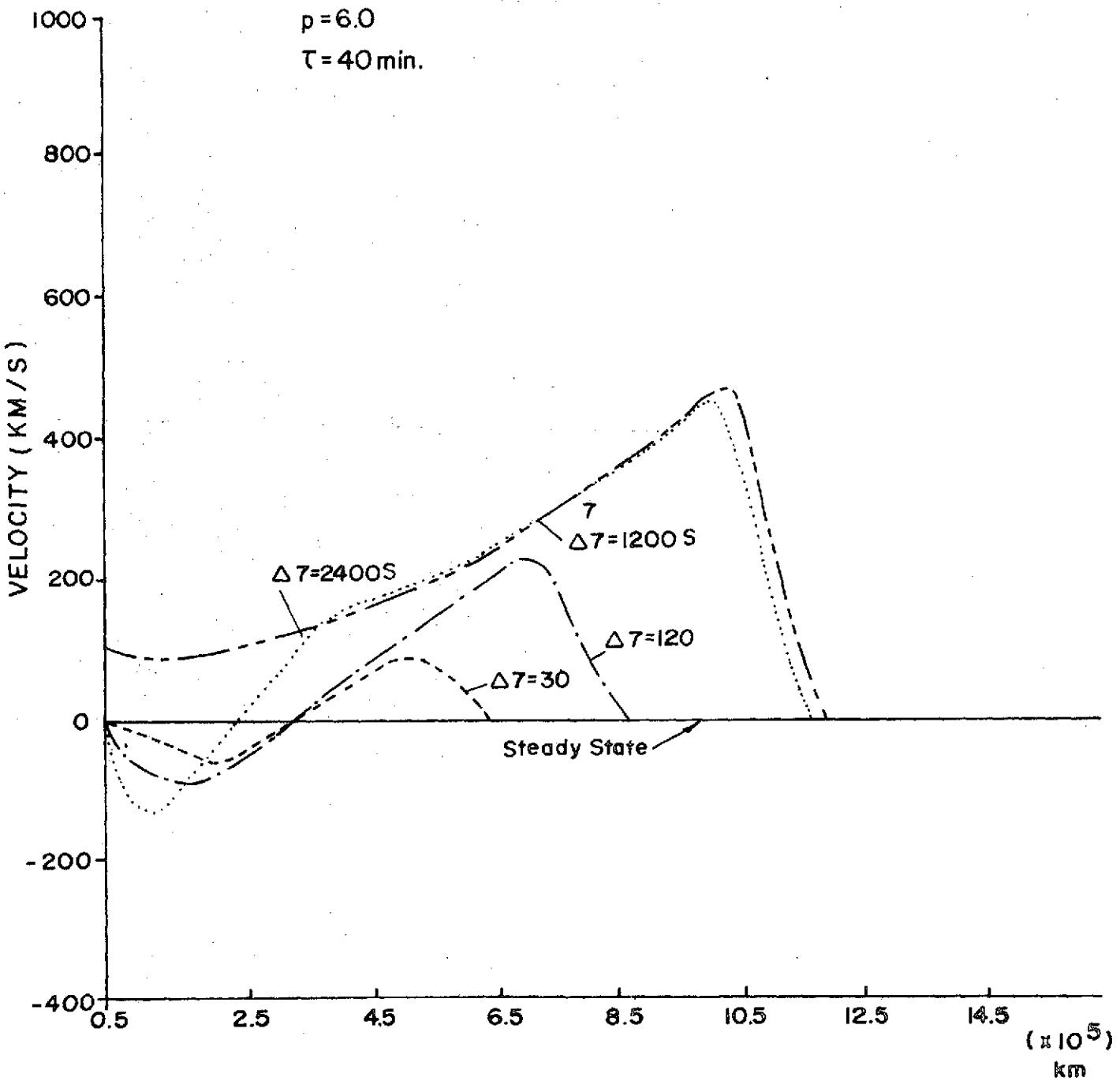
p = 6.0
τ = 40 min.
1000
800
600
400
200
0
-200
-400
VELOCITY (KM / S)
Δ7=2400S
Δ7=1200 S
Δ7=120
Δ7=30
Steady State
0.5
2.5
4.5
6.5
8.5
10.5
12.5
14.5
(x 10^5)
km

FIG. 12

APPENDIX A

Derivation of Conservational Form of Equations

The governing equations for the present problem written in spherical coordinates are

Continuity;
$$\frac{\partial \rho}{\partial t} = - \frac{\partial}{\partial r} (\rho u) - \frac{2\rho u}{r} . \qquad \text{(A-1)}$$

Momentum;
$$\frac{\partial u}{\partial t} = - u\frac{\partial u}{\partial r} - \frac{1}{\rho} \frac{\partial P}{\partial r} - g . \qquad \text{(A-2)}$$

Energy;
$$\rho \frac{\partial \varepsilon}{\partial t} = - \rho u \frac{\partial \varepsilon}{\partial r} + \frac{P}{\rho} \left(\frac{\partial \rho}{\partial t} + u \frac{\partial \rho}{\partial r}\right) - Q_R,$$ but by virtue of Equation (A-1), this can be written

$$\rho \frac{\partial \varepsilon}{\partial t} = -\rho u \frac{\partial \varepsilon}{\partial r} - p \frac{\partial u}{\partial r} - p \frac{2u}{r} - Q_R \qquad \text{(A-3)}$$

Continuity equation (A-1) is already in conservational form. Multiplying ρ to equation (A-2) and rearranging with the aid of equation (A-1), we have momentum conservational form of equations,

$$\frac{\partial (\rho u)}{\partial t} = - \frac{\partial}{\partial r} (\rho u^2 + p) - \rho g - \frac{2\rho u^2}{r} , \qquad \text{(A-4)}$$

noting however $p = (\gamma-1)E - \frac{(\gamma-1)}{2} \rho u^2$ by definition, equation (A-4) becomes

$$\frac{\partial (\rho u)}{\partial t} = - \frac{\partial}{\partial r} \left[(\gamma-1)E - \frac{(\gamma-3)}{2} \rho u^2\right] - \rho g - \frac{2\rho u^2}{r} \qquad \text{(A-5)}$$

Energy conservational form is found by adding four equations, i.e., ε x eqn. (A-1), $\frac{\rho u}{2}$ x eqn. (A-2), $\frac{u}{2}$ x eqn. (A-4) and eqn. (A-3).

Collecting $\partial/\partial t$ terms, we have after some simplification,

$$\frac{\partial}{\partial t}\left(\rho\varepsilon + \frac{\rho u^2}{2}\right) = \frac{\partial E}{\partial t} \tag{A-6}$$

Collecting $\partial/\partial r$ terms and other remaining terms, we get, after some simplifications,

$$-\frac{\partial}{\partial r}\left[u\left(p + \rho\varepsilon + \frac{\rho u^2}{2}\right)\right] - u\rho g - \frac{2u}{r}\left[\rho\varepsilon + \frac{\rho u^2}{2} + p\right] - Q_R$$

$$= -\frac{\partial}{\partial r}\left[u\left(\gamma E - \frac{(\gamma-1)}{2}\rho u^2\right)\right] - \rho g u - Q_R - \frac{2}{r}\left[u\left(rE - \frac{(\gamma-1)}{2}\rho u^2\right)\right] \tag{A-7}$$

Thus, energy conservational form of equation is

$$\frac{\partial E}{\partial t} = -\frac{\partial}{\partial r}\left[u\left(\gamma E - \frac{(\gamma-1)}{2}\rho u^2\right)\right] - \rho g u - Q_R - \frac{2}{r}\left[u\left(\gamma E - \frac{(\gamma-1)}{2}\rho u^2\right)\right] \tag{A-8}$$

APPENDIX B

COMPUTER LISTING

```
      C
      C     ONE DIMENSIONAL MOVING SHOCH THROUGH THE SOLAR ATMOSPHERE
      C     95 INVESTIGATED BY UTILIZING FINITE DIFFERENCE TECHNIQUE
      C     BASED ON THE LAX-WENDROFF CONSERVATIONAL LAW.
      C     THE FINAL DIFFERENCE SCHEME IS BASED ON RUBIN-BURSTEIN,S METHOD.
      C
            PARAMETER IMAX=40
            PARAMETER JMAX=5
            REAL K1,K2,K3
            REAL K1H,K2H,K3H
            REAL K1A,K1B,K2A,K2B,K3A,K3B
            COMMON/BLOC1/IM1,IM2
            COMMON/BLOC2/GAM,GAM1,GAM3,GSRS,CI,R
            COMMON/BLOC3/RX(IMAX),X(IMAX),PHI(IMAX),RXSQ(IMAX)
            COMMON/BLOC4/F1(IMAX),F2(IMAX),F3(IMAX),K2(IMAX),K3(IMAX)
           1,K1(IMAX)
            COMMON/BLOC5/U1(IMAX),U2(IMAX),U3(IMAX)
            COMMON/BLOC20/UU(IMAX),TE(IMAX)
            COMMON/BLOC6/U3Q,TEQ,U2Q,UUQ,U1Q
            COMMON/BLOC7/U1I,U2I,UUI,U3I,TEI
            COMMON/BLOC8/TEC(IMAX),U1C(IMAX)
            COMMON/BLOC9/U1P(JMAX,IMAX),UUP(JMAX,IMAX),TEP(JMAX,IMAX)
            COMMON/BLOC10/HX(IMAX),CX(IMAX)
            COMMON/BLOC11/ U1A(IMAX),U2A(IMAX),U3A(IMAX),U1B(IMAX),
           1U2B(IMAX),U3B(IMAX)
            COMMON/BLOC12/ F1A(IMAX),F2A(IMAX),F3A(IMAX),F1B(IMAX),
           1F2B(IMAX),F3B(IMAX)
            COMMON/BLOC13/U1H(IMAX),U2H(IMAX),UUH(IMAX),TEH(IMAX)
            COMMON/BLOC14/K1H(IMAX),K2H(IMAX),K3H(IMAX)
            COMMON/BLOC15/U3H(IMAX),UUA(IMAX),UUB(IMAX)
            COMMON/BLOC16/DT
            COMMON/BLOC26/C(IMAX)
            COMMON/BLOC30/EI(IMAX)
            COMMON/BLOC25/K1A(IMAX),K1B(IMAX),K2A(IMAX),K2B(IMAX),K3A(IMAX)
           1,K3B(IMAX)
            COMMON/BLOC33/U3C(IMAX),UUC(IMAX)
            COMMON/BLOC42/QR(IMAX)
            COMMON/BLOC43/QRC(IMAX)
            COMMON/BLOC50/T
      C     GAM=SPECIFIC HEAT RATIO
      C     RS=RADIUS OF THE SUN
      C     HP=HEIGHT OF THE PROMINENCE
      C     HC=HEIGHT O F THE CHROMOSPHERE
      C     GS=GRAVITATIONAL ACC.AT THE SURFACE OF THE SUN
      C     DX=SPATIAL INCREAMENT
      C     R=GAS CONSTANT
      C     DT=TIME INCREAMENT
      C     DTP=TIME INCREAMENT TO RECORD DATAS ON THE MAGNETIC TAPE
      C     U1C=UNPERTURBED CORONA DENSITY AT THE SURFACE OF THE SUN
      C     VARIABE NAMES
      C     U1=DENSITY
      C     U2=MOMENTUM DENSITY
      C     UU=VELOCITY
      C     X=SPATIAL COORDINATE MEASURED UPWARD
      C     Z=SPATIAL COORDINATE MEASURED DOWNWARD
      C     SDT=SHOCK DURATION TIME AT THE LOWER BOUNDARY.
            READ (5,10) TSTOP
```

```
      READ (5,66) (X(I),TE(I),U1(I),I=1,1)
      IM1=IMAX-1
      IM2=IMAX-2
      GAM=5./3.
      GAM1=GAM-1.
      GAM3=3.-GAM
      RS=.695E+6
      HP=7.E5
      HC=3.E4
      GS=.274
      R=.83E-2
      DTP=480.
      SDT=600.
      C1=GAM1/R
      GSRS=GS*RS**2
      U10=4.14713E8
C
C     INITIALIZATION
C
      RX(1)=RS+HC
      T=0.
      TP=0.
      DO 20 I=1,1
      RX(I)=X(I)+RS
      RXSQ(I)=RX(I)**2
   20 CONTINUE
      DO 77 I=2,IMAX
      X(I)=X(I-1)+2.0000.
      RX(I)=X(I)+RS
      RXSQ(I)=RX(I)**2
      TE(I)=1.53E6
      U1(I)=U10*EXP((GSRS/(R*TE(I)))*(1./RX(I) -1./RX(1)))
   77 CONTINUE
      DO 60 I=1,IMAX
      CON=2.E-12
      U1(I)=CON*U1(I)
      UU(I)=0.
      U2(I)=U1(I)*UU(I)
      PHI(I)=+GSRS/RX(I)
      U3(I)=U1(I)*(TE(I)/C1+.5*UU(I)**2)
      C(I)=SQRT(GAM*R*TE(I))
      E1(I)=U1(I)*TE(I)/C1
      U1C(I)=U1(I)
      U3C(I)=U3(I)
      TEC(I)=TE(I)
   60 CONTINUE
      DO 111 I=2,IM1
      HX(I)=GSRS/(R*TE(I))*((X(I+1)-X(I))/RXSQ(I))
      CX(I)= (HX(I)+.5*(EXP(-HX(I))-EXP(HX(I))))/(X(I+1)-X(I))
  111 CONTINUE
      WRITE (6,10) T
      WRITE (6,105)
      WRITE (6,110) (X(I),I=1,IMAX)
      WRITE (6,105)
      WRITE (6,110) (U1(I),I=1,IMAX)
      WRITE (6,105)
      WRITE (6,110) (UU(I),I=1,IMAX)
      WRITE (6,105)
```

```
116*            WRITE (6,115) (U3(I),I=1,IMAX)
117*            WRITE (6,105)
118*            WRITE (6,110) (TE(I),I=1,IMAX)
119*            WRITE (6,105)
120*            WRITE (6,110) (PHI(I),I=1,IMAX)
121*            WRITE (6,120)
122*      C
123*      C     BACKGROUND CORONA RADIATION IS DETERMINED BY TUCKER'S EQN.....
124*      C     RADIATION EFFECTS ARE INTRODUCED BY INCLUDING RADIATION EQN
125*      C     OBTAINED BY FITTING OF TUCKER,S RESULTS.
126*      C
127*            DO 62 I=1,IMAX
128*            IF (TE(I).GT.5.0E4) GO TO 11
129*            C2=1.0E10
130*            C3=3.59
131*            GO TO 79
132*         11 IF (TE(I).GT.2.5E5) GO TO 12
133*            C2=3.0E26
134*            C3=0.
135*            GO TO 79
136*         12 IF (TE(I).GT.7.0E6) GO TO 13
137*            C2=1.0E32
138*            C3=-1.172
139*            GO TO 79
140*         13 C2=1.0E23
141*            C3=0.288
142*         79 QRC(I)=C2*(U1(I)**2)*(TE(I)**C3)
143*         62 CONTINUE
144*      C
145*      C
146*      C     PLOTTING OF THE INITIAL VALUES OF THE VARIABLES....
147*      C
148*            CALL PLOT (0,U1,UU,TE)
149*            TP=TP+DTP
150*            U1I=U1(1)
151*            U2I=U2(1)
152*            UUI=UU(1)
153*            U3I=U3(1)
154*            TEI=TE(1)
155*      C
156*      C
157*      C     UPWARD PROPAGATING SHOCK SIMULATION IN TERMS OF DENSITY,
158*      C     ENERGY,TEMPERATURE GRADIENT.....
159*      C     REFLECTED SHOCK MACH NUMBERS ARE ASSUMED TO BE KNOWN
160*      C     AT THE LOWER BOUNDARY. THEN THE JUMP CONDITUONS ARE FOUND BY
161*      C     RANKINE-HUGONIOT RELATIONS.
162*      C
163*            U10=U1(1)*2.
164*            UU0=0.
165*            U20=U10*UU0
166*            TE0=TE(1)
167*            U30=U10*(TE0/C1+.5*UU0**2)
168*      C
169*            KW=1
170*            U1(1)=U10
171*            UU(1)=UU0
172*            U2(1)=U20
173*            U3(1)=U30
```

```
174*            TE(I)=TEU
175*            C(I)=SQRT(GAM*R*TE(I))
176*            EI(I)=U1(I)*TE(I)/C1
177*         70 CONTINUE
178*      C
179*      C     PREDICTOR STEP.....
180*      C
181*            CALL DTIME (UU,C )
182*            IF (DT.LT.0.01) GO TO 200
183*            IF (T.LT.30.) DT=1.
184*            SDD=SDT+30.
185*            IF (T.GT.SDT.AND.T.LT.SDD) DT=1.
186*            CALL FLUX1 (U1,U2,U3,TE,UU,C)
187*            CALL EQN1 (U1,U2,U3,F1,F2,F3,K2,K3,DT,CX,HX,K1)
188*      C
189*      C     CORRECTOR STEP
190*      C
191*            CALL FLUX2 (U1A,U1B,U2A,U2B,U3A,U3B,U1H,U2H,U3H,TEH,UU,C,
192*           1UUA,UUB,UUH,U1)
193*            CALL EQN2 (U1,U2,U3,F1,F2,F3,K2,K3,F1A,F2A,F3A,K1,K1H,E1,
194*           1F1B,F2B,F3B,K2H,K3H,DT,CX,HX,K1A,K1B,K2A,K2B,K3A,K3B)
195*            T=T+DT
196*      C
197*      C     REFLECTED SHOCK SIMULATION IN TERM OF THE KNOWN MACH NUMBER.
198*      C
199*            CALL BOUND
200*      C
201*            IF (KW.GT.0 ) GO TO 555
202*            GO TO 666
203*        555 CONTINUE
204*            WRITE (6,10) T
205*            WRITE (6,105)
206*            WRITE (6,110) (U1(I),I=1,IMAX)
207*            WRITE (6,105)
208*            WRITE (6,110) (UU(I),I=1,IMAX)
209*            WRITE (6,105)
210*            WRITE (6,110) (U3(I),I=1,IMAX)
211*            WRITE (6,105)
212*            WRITE (6,110) (TE(I),I=1,IMAX)
213*            WRITE (6,105)
214*            WRITE (6,110) (EI(I),I=1,IMAX)
215*            WRITE (6,120)
216*            DO 404 I=1,IMAX
217*            C(I)=SQRT(GAM*R*TE(I))
218*        404 CONTINUE
219*            KW=0
220*        666 CONTINUE
221*            KW=KW+1
222*      C
223*      C     PLOTTING OF THE PRRTURBED VARIABLES.....
224*      C
225*            IF (T.GT.TP) GO TO 150
226*            GO TO 160
227*        150 CONTINUE
228*            CALL PLOT (I,U1,UU,TE)
229*            TP=TP+DTP
230*        160 IF (T.GT.TSTOP) GO TO 200
231*            GO TO 70
```

```
232*        200 CONTINUE
233*      C
234*            K=1
235*            DO 190 I=1,IMAX
236             X(K)=X(I)
237*            K=K+1
238*      C
239*        190 CONTINUE
240*      C
241*      C     THE FOLLOWING IS TO RECORD THE DATAS ON THE TAPE....
242*      C
243*            DO 210 J=1,JMAX
244*            DO 210 I=1,IMAX
245*            IF (I.EQ.IMAX) X(I)=1.0E37
246*            IF (I.EQ.IMAX) UIP(J,I)=1.0E37
247*            IF (I.EQ.IMAX.AND.J.EQ.JMAX) X(I)=9.0E37
248*            IF (I.EQ.IMAX.AND.J.EQ.JMAX) UIP(J,I)=9.0E37
249*            WRITE (9) X(I),UIP(J,I)
250*        210 CONTINUE
251*            DO 300 J=1,JMAX
252*            DO 300 I=1,IMAX
253*            IF (I.EQ.IMAX) X(I)=1.0E37
254*            IF (I.EQ.IMAX) UUP(J,I)=1.0E37
255*            IF (I.EQ.IMAX.AND.J.EQ.JMAX) X(I)=9.0E37
256*            IF (I.EQ.IMAX.AND.J.EQ.JMAX) UUP(J,I)=9.0E37
257*            WRITE (9) X(I),UUP(J,I)
258*        300 CONTINUE
259*            DO 400 J=1,JMAX
260*            DO 400 I=1,IMAX
261             IF (I.EQ.IMAX) X(I)=1.0E37
262*            IF (I.EQ.IMAX) TEP(J,I)=1.0E37
263*            IF (I.EQ.IMAX.AND.J.EQ.JMAX) X(I)=9.0E37
264*            IF (I.EQ.IMAX.AND.J.EQ.JMAX) TEP(J,I)=9.0E37
265*            WRITE (9) X(I),TEP(J,I)
266*        400 CONTINUE
267*            STOP
268*         10 FORMAT (E15.4)
269*         66 FORMAT (2F15.4,E15.6)
270*        105 FORMAT (1H  )
271*        110 FORMAT (1X, 9E11.4)
272*        120 FORMAT (1H1)
273*            END
```

NO OF COMPILATION: NO DIAGNOSTICS.

```
1*              SUBROUTINE FLUX1 (U1,U2,U3,TE,UU,C)
2*              PARAMETER IMAX=46
3*              REAL K1,K2,K3
4*              COMMON/BLOC1/IM1,IM2
5*              COMMON/BLOC2/GAM,GAM1,GAM3,GSRS,C1,R
6*              COMMON/BLOC3/RX(IMAX),X(IMAX),PHI(IMAX),RXSQ(IMAX)
7*              COMMON/BLOC4/F1(IMAX),F2(IMAX),F3(IMAX),K2(IMAX),K3(IMAX)
8*             1,K1(IMAX)
9*              COMMON/BLOC8/TEC(IMAX),U1C(IMAX)
10*             COMMON/BLOC16/DT
11*             COMMON/BLOC42/QR(IMAX)
12*             COMMON/BLOC43/QRC(IMAX)
13*             DIMENSION U1(IMAX),U2(IMAX),U3(IMAX),TE(IMAX)
14*             DIMENSION UU(IMAX),C(IMAX),QD(IMAX),DM(IMAX)
15*             DIMENSION UD(IMAX)
16*     C
17*     C       C2 AND C3 ARE CONSTANTS USED IN TUCKER'S RADIATION EQN.
18*     C       CO=CONVERSION FACTOR
19*     C
20*             CO=1.0E-22
21*             AC=3.
22*     C
23*     C       RADIATION EFFECTS ARE INTRODUCED BY INCLUDING RADIATION EQN
24*     C       OBTAINED BY FITTING OF TUCKER,S RESULTS.
25*             DO 60 I=1,IMAX
26*             IF (TE(I).GT.5.0E4) GO TO 11
27*             C2=1.0E10
28*             C3=3.55
29*             GO TO 77
30*          11 IF (TE(I).GT.2.5E5) GO TO 12
31*             C2=3.0E26
32*             C3=0.
33*             GO TO 77
34*          12 IF (TE(I).GT.7.0E6) GO TO 13
35*             C2=1.0E32
36*             C3=-1.172
37*             GO TO 77
38*          13 C2=1.0E23
39*             C3=0.288
40*          77 QR(I)=C2*(U1(I)**2)*(TE(I)**C3)*CO
41*          60 CONTINUE
42*             DO 88 I=2,IM1
43*             QR(I)=-QR(I)+.5*(.5*(QR(I+1)+QR(I-1))+QRC(I)*CO)
44*          88 CONTINUE
45*             QR(1)=.5*(-QR(1)+.5*(QR(2)+QR(1))+QRC(1)*CO)
46*             QR(IMAX)=.5*(-QR(IMAX)+.5*(QR(IMAX)+QR(IM1))+QRC(IMAX)*CO)
47*     C
48*             DO 66 I=2,IM1
49*             UD(I)=UU(I)-UU(I-1)
50*          66 CONTINUE
51*             DO 20 I=2,IM1
52*             IF (UD(I).GT.0.) GO TO 30
53*             GO TO 20
54*          30 UD(I)=0.
55          20 CONTINUE
56*             UD(1)=0.
57*             UD(IMAX)=0.
```

```
      C
      C
            DO 50 I=2,IM1
            DM(I)=UU(I-1)/C(I  )-UU(I)/C(I)
            IF (DM(I).GT.1.0) GO TO 80
            QD(I)=0.
            GO TO 50
         80 CONTINUE
            SM=DM(I)
            PAI=(2.*GAM/(GAM+1.))*(SM**2)-(GAM1/(GAM+1.))
            SIG=(GAM+1.)*(SM**2)/(GAM1*SM**2+2.)
            ZETA=SQRT(PAI/SIG)
            QD(I)=U1 (I)*(C(I)**2)*(.5*(PAI-1.)*(1./SIG+1.)
           1-(GAM/GAM1)*(ZETA**2+1.))/(DT*GAM)
            QD(I)=ABS(QD(I))
         50 CONTINUE
            QD(1)=0.
            QD(IMAX)=0.
      C
            DO 10 I=1,IMAX
            F1(I)=U2(I)
            F2(I)=GAM1*U3(I)+0.5*GAM3*U2(I)**2/U1(I)
           1+.5*(AC**2)*U1(I)*(UD(I)**2)
            F3(I)=(U2(I)/U1(I))*(GAM*U3(I)-.5*GAM1*U2(I)**2/U1(I)
           1+.5*(AC**2)*U1(I)*(UD(I)**2))
            K1(I)=-2.*U2(I)/RX(I)
            K2(I)=-U1(I)*GSRS/RXSQ(I)
           1-2.*U2(I)**2/(RX(I)*U1(I))
            K3(I)=-U2(I)*GSRS/RXSQ(I)
           2-2.*U2(I)*(GAM*U3(I)-GAM1*.5*U2(I)**2/U1(I)
           3+.5*(AC**2)*U1(I)*(UD(I)**2))/(RX(I)*U1(I))
           4+QD(I)
         10 CONTINUE
            RETURN
            END

D OF COMPILATION:        NO  DIAGNOSTICS.


            SUBROUTINE EQN1 (U1,U2,U3,F1,F2,F3,K2,K3,DT,CX,HX,K1)
            PARAMETER IMAX=40
            REAL K1,K2,K3
            COMMON/BLOC1/IM1,IM2
            COMMON/BLOC2/GAM,GAM1,GAM3,GSRS,C1,R
            COMMON/BLOC3/RX(IMAX),X(IMAX),PHI(IMAX),RXSQ(IMAX)
            COMMON/BLOC11/ U1A(IMAX),U2A(IMAX),U3A(IMAX),U1B(IMAX),
           1U2B(IMAX),U3B(IMAX)
            COMMON/BLOC12/ F1A(IMAX),F2A(IMAX),F3A(IMAX),F1B(IMAX),
           1F2B(IMAX),F3B(IMAX)
            COMMON/BLOC13/U1H(IMAX),U2H(IMAX),UUH(IMAX),TEH(IMAX)
            COMMON/BLOC14/K1H(IMAX),K2H(IMAX),K3H(IMAX)
            COMMON/BLOC15/U3H(IMAX),UUA(IMAX),UUB(IMAX)
            DIMENSION HX(IMAX),CX(IMAX)
            DIMENSION F1(IMAX),F2(IMAX),F3(IMAX),K2(IMAX),K3(IMAX),K1(IMAX)
            DIMENSION U1(IMAX),U2(IMAX),U3(IMAX)
```

```
      DO 50 I=2,IM1
      U1A(I)=.5*(U1(I+1)+U1(I))-(DT/(X(I+1)-X(I)))*(F1(I+1)-F1(I))+
     1.5*DT*(K1(I+1)+K1(I))
      U2A(I)=.5*(U2(I+1)+U2(I))-(DT/(X(I+1)-X(I)))*(F2(I+1)-F2(I))+
     1(.5*DT)*(K2(I+1)+K2(I))
      U3A(I)=.5*(U3(I+1)+U3(I))-(DT/(X(I+1)-X(I)))*(F3(I+1)-F3(I))+
     1(.5*DT)*(K3(I+1)+K3(I))
      U1B(I)=.5*(U1(I-1)+U1(I))+(DT/(X(I)-X(I-1)))*(F1(I-1)-F1(I))+
     1.5*DT*(K1(I-1)+K1(I))
      U2B(I)=.5*(U2(I-1)+U2(I))+(DT/(X(I)-X(I-1)))*(F2(I-1)-F2(I))+
     1(.5*DT)*(K2(I-1)+K2(I))
      U3B(I)=.5*(U3(I-1)+U3(I))+(DT/(X(I)-X(I-1)))*(F3(I-1)-F3(I))+
     1(.5*DT)*(K3(I-1)+K3(I))
      U1H(I)=.5*(U1(I+1)+U1(I-1))-(DT/(X(I+1)-X(I-1)))*(F1(I+1)
     1-F1(I-1)) +
     2DT*K1(I)
     2+DT*CX(I)*F1(I)
     3+.5*U1(I)*(1.-.5*(EXP(-HX(I))+EXP(HX(I))))
      U2H(I)=.5*(U2(I+1)+U2(I-1))-(DT/(X(I+1)-X(I-1)))*(F2(I+1)
     1-F2(I-1)) +
     2DT*K2(I)
     2+DT*CX(I)*F2(I)
     3+.5*U2(I)*(1.-.5*(EXP(-HX(I))+EXP(HX(I))))
      U3H(I)=.5*(U3(I+1)+U3(I-1))-(DT/(X(I+1)-X(I-1)))*(F3(I+1)
     1-F3(I-1)) +
     2DT*K3(I)
     2+DT*CX(I)*F3(I)
     3+.5*U3(I)*(1.-.5*(EXP(-HX(I))+EXP(HX(I))))
      UUA(I)=U2A(I)/U1A(I)
      UUB(I)=U2B(I)/U1B(I)
      UUH(I)=U2H(I)/U1H(I)
      TEH(I)=C1*(U3H(I)/U1H(I)-.5*UUH(I)**2)
   50 CONTINUE
      RETURN
      END
```

```
ID OF COMPILATION:        NO  DIAGNOSTICS.
```

```
      SUBROUTINE FLUX2 (U1A,U1B,U2A,U2B,U3A,U3B,U1H,U2H,U3H,TEH,UU,C,
     1UUA,UUB,UUH,U1)
      PARAMETER IMAX=40
      REAL K1H,K2H,K3H
      REAL K1A,K1B,K2A,K2B,K3A,K3B
      COMMON/BLOC1/IM1,IM2
      COMMON/BLOC2/GAM,GAM1,GAM3,GSRS,C1,R
      COMMON/BLOC3/RX(IMAX),X(IMAX),PHI(IMAX),RXSQ(IMAX)
      COMMON/BLOC8/TEC(IMAX),UIC(IMAX)
      COMMON/BLOC12/ F1A(IMAX),F2A(IMAX),F3A(IMAX),F1B(IMAX),
     1F2B(IMAX),F3B(IMAX)
```

```
12*           COMMON/BLOC14/K1H(IMAX),K2H(IMAX),K3H(IMAX)
13*           COMMON/BLOC25/K1A(IMAX),K1B(IMAX),K2A(IMAX),K2B(IMAX),K3A(IMAX)
14*          1,K3B(IMAX)
15*           COMMON/BLOC16/DT
16*           COMMON/BLOC42/QR(IMAX)
17*           DIMENSION U1A(IMAX),U2A(IMAX),U3A(IMAX),U1B(IMAX),U2B(IMAX),
18*          1U3B(IMAX),U1H(IMAX),U2H(IMAX),U3H(IMAX),TEH(IMAX)
19*           DIMENSION UU(IMAX),UD(IMAX)
20*           DIMENSION C(IMAX),DM(IMAX),QD(IMAX)
21*           DIMENSION UDA(IMAX),UDB(IMAX),UUA(IMAX),UUB(IMAX)
22*           DIMENSION UUH(IMAX)
23*           DIMENSION U1(IMAX)
24*           AC=3.
25*           DO 66 I=2,IM1
26*           UD (I)=UU(I)-UU(I-1)
27*           UDA(I)=(UU(I+1)-UU(I))/2.
28*           UDB(I)=(UU(I)-UU(I-1))/2.
29*        66 CONTINUE
30*           DO 20 I=2,IM1
31*           IF (UD (I).GT.0. ) GO TO 30
32*           GO TO 20
33*        30 UD (I)=0.
34*        20 CONTINUE
35*           DO 21 I=2,IM1
36*           IF (UDA(I).GT.0. ) GO TO 31
37*           GO TO 21
38*        31 UDA(I)=0.
39*        21 CONTINUE
40*           DO 22 I=2,IM1
41*           IF (UDB(I).GT.0. ) GO TO 32
42*           GO TO 22
43*        32 UDB(I)=0.
44*        22 CONTINUE
45*     C
46*           DO 50 I=2,IM1
47*           DM(I)=UU(I-1)/C(I   )-UU(I)/C(I)
48*           IF (DM(I).GT.1.0) GO TO 80
49*           QD(I)=0.
50*           GO TO 50
51*        80 CONTINUE
52*           SM=DM(I)
53*           PAI=(2.*GAM/(GAM+1.))*(SM**2)-(GAM1/(GAM+1.))
54*           SIG=(GAM+1.)*(SM**2)/(GAM1*SM**2+2.)
55*           ZETA=SQRT(PAI/SIG)
56*           QD(I)=U1 (I)*(C(I)**2)*(.5*(PAI-1.)*(1./SIG+1.)
57*          1-(GAM/GAM1)*(ZETA**2+1.))/(DT*GAM)
58*           QD(I)=ABS(QD(I))
59*        50 CONTINUE
60*     C
61*           DO 10 I=2,IM1
62*           F1A(I)=U2A(I)
63*           F2A(I)=GAM1*U3A(I)+.5*GAM3*U2A(I)**2/U1A(I)
64*          1+.5*(AC**2)*U1A(I)*(UDA(I)**2)
65*           F3A(I)=(U2A(I)/U1A(I))*(GAM*U3A(I)-.5*GAM1*U2A(I)**2/U1A(I)
66*          1+.5*(AC**2)*U1A(I)*(UDA(I)**2))
67*           F1B(I)=U2B(I)
68*           F2B(I)=GAM1*U3B(I)+.5*GAM3*U2B(I)**2/U1B(I)
```

```
     1+.5*(AC**2)*U1B(I)*(UDB(I)**2)
      F3B(I)=(U2B(I)/U1B(I))*(GAM*U3B(I)-.5*GAM1*U2B(I)**2/U1B(I)
     1+.5*(AC**2)*U1B(I)*(UDB(I)**2) )
      K1H(I)=-2.*U2H(I)/RX(I)
      K2H(I)=-U1H(I)*GSRS/RXSQ(I)
     1-2.*U2H(I)**2/(RX(I)*U1H(I))
      K3H(I)=-U2H(I)*GSRS/RXSQ(I)
     2-2.*U2H(I)*(GAM*U3H(I)-GAM1*.5*U2H(I)**2/U1H(I)
     3+.5*(AC**2)*U1H(I)*(UD(I)**2))/(RX(I)*U1H(I))
     4+QD(I)
      K1A(I)=-2.*U2A(I)/RX(I)
      K1B(I)=-2.*U2B(I)/RX(I)
      K2A(I)=-U1A(I)*GSRS/RXSQ(I)
     1-2.*U2A(I)**2/(RX(I)*U1A(I))
      K2B(I)=-U1B(I)*GSRS/RXSQ(I)
     1-2.*U2B(I)**2/(RX(I)*U1B(I))
      K3A(I)=-U2A(I)*GSRS/RXSQ(I)
     2-2.*U2A(I)*(GAM*U3A(I)-GAM1*.5*U2A(I)**2/U1A(I)
     3+.5*(AC**2)*U1A(I)*(UD(I)**2))/(RX(I)*U1A(I))
      K3B(I)=-U2B(I)*GSRS/RXSQ(I)
     2-2.*U2B(I)*(GAM*U3B(I)-GAM1*.5*U2B(I)**2/U1B(I)
     3+.5*(AC**2)*U1B(I)*(UD(I)**2))/(RX(I)*U1B(I))
   10 CONTINUE
      RETURN
      END
```

```
 OF COMPILATION:          NO  DIAGNOSTICS.
```

```
      SUBROUTINE EQN2(U1,U2,U3,F1,F2,F3,K2,K3,F1A,F2A,F3A,K1,K1H,E1,
     1F1B,F2B,F3B,K2H,K3H,DT,CX,HX,K1A,K1B,K2A,K2B,K3A,K3B)
      PARAMETER IMAX=40
      REAL K1,K2,K3
      REAL K1H,K2H,K3H
      REAL K1A,K1B,K2A,K2B,K3A,K3B
      COMMON/BLOC1/IM1,IM2
      COMMON/BLOC2/GAM,GAM1,GAM3,GSRS,CI,R
      COMMON/BLOC3/RX(IMAX),X(IMAX),PHI(IMAX),RXSQ(IMAX)
      COMMON/BLOC6/U30,TE0,U20,UU0,U10
      COMMON/BLOC7/U11,U21,UU1,U31,TE1
      COMMON/BLOC8/TEC(IMAX),U1C(IMAX)
      COMMON/BLOC20/UU(IMAX),TE(IMAX)
      COMMON/BLOC33/U3C(IMAX),UUC(IMAX)
      DIMENSION HX(IMAX),CX(IMAX)
      DIMENSION F1(IMAX),F2(IMAX),F3(IMAX),K2(IMAX),K3(IMAX),K1(IMAX)
      DIMENSION F1A(IMAX),F2A(IMAX),F3A(IMAX),F1B(IMAX),F2B(IMAX),
```

```
18*           1F3B(IMAX),K2H(IMAX),K3H(IMAX),K1H(IMAX)
19*            DIMENSION U1(IMAX),U2(IMAX),U3(IMAX)
20*            DIMENSION K1A(IMAX),K1B(IMAX),K2A(IMAX),K2B(IMAX)
21*           1,K3A(IMAX),K3B(IMAX)
22*            DIMENSION E1(IMAX)
23*            DIMENSION E1T(IMAX),E1E(IMAX)
24*            DO 48 I=2,IM1
25*         48 E1T(I)=E1(I)
26*            DO 50 I=2,IM1
27*            U1(I)=U1(I)-(DT/(X(I+1)-X(I-1)))*(.5*(F1(I+1)-F1(I-1))
28*           1+(F1A(I)-F1B(I)))
29*           2+DT*.5*(K1(I)+K1H(I))
30*           2+DT*CX(I)*F1(I)
31*            U2(I)=U2(I)-(DT/(X(I+1)-X(I-1)))*(.5*(F2(I+1)-F2(I-1))
32*           1+(F2A(I)-F2B(I)))
33*           2+DT*.5*(K2(I)+K2H(I))
34*           2+DT*CX(I)*F2(I)
35*            U3(I)=U3(I)-(DT/(X(I+1)-X(I-1)))*(.5*(F3(I+1)-F3(I-1))
36*           1+(F3A(I)-F3B(I)))
37*           2+DT*.5*(K3(I)+K3H(I))
38*           2+DT*CX(I)*F3(I)
39*            UU(I)=U2(I)/U1(I)
40*            TE(I)=C1*(U3(I)/U1(I)-.5*UU(I)**2)
41*            E1(I)=U1(I)*TE(I)/C1
42*         50 CONTINUE
43*      C
44*            DO 47 I=2,IM1
45*            E1E(I)=(E1T(I)-E1(I))/E1T(I)
46*            IF (E1E(I).LT.0.50) GO TO 47
47*            E1(I)=0.50*E1T(I)
48*            TE(I)=E1(I)*C1/U1(I)
49*            U3(I)=U1(I)*(TE(I)/C1+.5*UU(I)**2)
50*         47 CONTINUE
51*      C
52*            RETURN
53*            END

D OF COMPILATION:          NO  DIAGNOSTICS.
```

```
1*              SUBROUTINE BOUND
2*              PARAMETER IMAX=40
3*              COMMON/BLOC1/IM1,IM2
4*              COMMON/BLOC2/GAM,GAM1,GAM3,GSRS,C1,R
5*              COMMON/BLOC5/U1(IMAX),U2(IMAX),U3(IMAX)
6*              COMMON/BLOC6/U30,TE0,U20,UU0,U10
7*              COMMON/BLOC7/U11,U21,UU1,U31,TE1
8*              COMMON/BLOC8/TEC(IMAX),U1C(IMAX)
9*              COMMON/BLOC20/UU(IMAX),TE(IMAX)
0*              COMMON/BLOC33/U3C(IMAX),UUC(IMAX)
1*              COMMON/BLOC50/T
2*              COMMON/BLOC30/EI(IMAX)
3*              SDT=600.
4*              IF (T.GT.SDT) GO TO 101
5*              U1(1)=U10
6*              U2(1)=U2(2)
7*              UU(1)=U2(1)/U1(1)
8*              TE(1)=TE0
9*              EI(1)=U1(1)*TE(1)/C1
0*              U3(1)=U1(1)*(TE(1)/C1+.5*UU(1)**2)
1*              GO TO 151
2*          101 CONTINUE
3*              U1(1)=U11
4*              TE(1)=TE1
5*              U2(1)=0.
6*              UU(1)=U2(1)/U1(1)
7*              EI(1)=U1(1)*TE(1)/C1
8*              U3(1)=U1(1)*(TE(1)/C1+.5*UU(1)**2)
9*          151 CONTINUE
0*      C
1*      C       UPPER BOUNDARY VALUE....
2*      C
3*              IF (UU(IM1).GT.20.) GO TO 150
4*              U1(IMAX)=U1C(IMAX)
5*              UU(IMAX)=UUC(IMAX)
6*              U2(IMAX)=U1(IMAX)*UU(IMAX)
7*              TE(IMAX)=TEC(IMAX)
8*              U3(IMAX)=U3C(IMAX)
9*              EI(IMAX)=U1(IMAX)*TE(IMAX)/C1
0*              GO TO 105
1*          150 U1(IMAX)=U1(IM1)
2*              U2(IMAX)=U2(IM1)
3*              U3(IMAX)=U3(IM1)
4*              UU(IMAX)=UU(IM1)
5*              TE(IMAX)=TE(IM1)
6*              EI(IMAX)=EI(IM1)
7*          105 CONTINUE
8*      C
9*              RETURN
0*              END

D OF COMPILATION:        NO  DIAGNOSTICS.
```

```
      SUBROUTINE PLOT (IFLAG,UI,UU,TE)
      PARAMETER IMAX=40
      PARAMETER JMAX=5
      COMMON/BLOC9/UIP(JMAX,IMAX),UUP(JMAX,IMAX),TEP(JMAX,IMAX)
      DIMENSION UI(IMAX),UU(IMAX),TE(IMAX)
      IF(IFLAG.EQ.1) GO TO 20
      J=1
      K=1
   20 CONTINUE
      DO 10 I=1,IMAX
      UIP(J,K)=UI(I)
      UUP(J,K)=UU(I)
      TEP(J,K)=TE(I)
      K=K+1
   10 CONTINUE
      J=J+1
      K=1
      RETURN
      END
```

```
ND OF COMPILATION:        NO  DIAGNOSTICS.
```

```
      SUBROUTINE DTIME (UU,C )
      PARAMETER IMAX=40
      COMMON/BLOC1/IM1,IM2
      COMMON/BLOC2/GAM,GAM1,GAM3,GSRS,C1,R
      COMMON/BLOC3/RX(IMAX),X(IMAX),PHI(IMAX),RXSQ(IMAX)
      COMMON/BLOC16/DT
      DIMENSION UU(IMAX), C(IMAX)
      DIMENSION DDT(IMAX)
      DO 10 I=1,IM1
      DDT(I)=.25*(X(I+1)-X(I))/(ABS(UU(I))+C(I))
   10 CONTINUE
      HDT=DDT(1)
      DO 20 I=2,IM1
      QDT=DDT(I)
      IF (HDT.GT.QDT) GO TO 30
      GO TO 20
   30 HDT=QDT
   20 CONTINUE
      DT=HDT
      RETURN
      END
```

```
ND OF COMPILATION:        NO  DIAGNOSTICS.
```

APPENDIX C

Presentations

During the period of performance of this contract, the following papers were presented.

(1) "A Compressible MHD Model of the Development of a Sunspot," Annual Meeting of the Solar Physics Division, American Astronomical Society, Huntsville, Alabama, November 17-19, 1970, with M. Hagyard and Y. Nakagawa.

(2) "H_α Flares: The Response of the Chromosphere to a Downward Shock Wave," Annual Meeting of the Solar Physics Division, American Astronomical Society, University of Maryland, April 4-6, 1972, with S. M. Han and Y. Nakagawa.

(3) "Non-Linear Study of the Dynamical Behavior of Force-Free Magnetic Field," Annual Meeting of the Solar Physics Division, American Astronomical Society, University of Maryland, April 4-6, 1972, with M. Hagyard and Y. Nakagawa.

(4) "Some Characteristics of Disturbed Solar Atmosphere," High Altitude Observatory Seminar (Invited), July 1973.

(5) "Solar Atmosphere," AIAA (American Institute of Aero. & Astro.)-Alabama Section Space and Atmospheric Sciences Panel Meeting, (Invited), December 3, 1973.